GeoExpert ag

swiss*nuclear*: PEGASOS Refinement Project:
SP2 – Ground Motion Characterization

Contract no. PMT-VT-1032

Seismic Shear Wave Velocity Determination and Hybrid Seismic Survey at the SED-Station STEIN (Stein am Rhein, SH)

Date of Field Data Acquisition 7th May 2009

Report

Client

swiss*nuclear*
Project PRP
Frohburgstrasse 17
4601 Olten

Contractor

GeoExpert ag
Seismic Prospecting
Ifangstrasse 12b
P.O. Box 451
8603 Schwerzenbach

8603 Schwerzenbach, 29th June 2009

INDEX

1 INTRODUCTION

1.1 Survey objectives

The seismic survey's main task is to provide information about the distribution function of the shear wave velocities in the depth interval of the uppermost 30 m along a 100 m long seismic profile.

Additionally, the following objectives are to be met:

- the mapping of the topography of the rock face, i.e. the thickness of the Quaternary deposits;
- the determination of the thickness of the weathered zone and its degree of decompaction at the bedrock surface;
- a general view of geological structures.

1.2 The choice of the appropriate surveying methods

Several methods are available for deriving the s-wave velocity distribution in the subsurface at any given position:

- in-situ measurement by down-hole or crosshole seismic surveying;
- shear-wave refraction tomography profiling;
- dispersion analysis of surface waves (MASW; **M**ultiple channel **A**nalysis of **S**urface **W**aves)

The surveys are to be carried out at, or as close as possible near some 20 SED earth quake monitoring stations in Switzerland. Ideally, the surveys are to be conducted on two orthogonal profiles in order to derive at their point of intersection a robust 1D s-wave velocity distribution function by correlation. To this end, the methods of MASW and shear-wave refraction tomography profiling are to be combined.

The results are to include the following fundamental parameters $v_{s,5}$, $v_{s,10}$, $v_{s,20}$, $v_{s,30}$, $v_{s,40}$, $v_{s,50}$, $v_{s,100}$ are to be calculated, also an error estimation of all values.

The data acquired for the MASW method are to be subjected to complementary **p-wave hybrid seismic data processing** in order to image the geological structures.

2 FIELD DATA ACQUISITION PARTICULARS

2.1 Time Schedule

Date	*Time*	*Activities / remarks*
07.05.2009	0845	arrival at site
	0845 - 0930	site investigation
	0930 - 1040	lay-out of spread profile 1 (p-wave and s-wave)
	1040 - 1125	data acquisition of spread profile 1 (p-wave)
	1140 - 1225	data acquisition of spread profile 1 (s-wave)
	1225 - 1330	lay-out of spread profile 2 (p-wave and s-wave)
	1330 - 1525	standby-due to work in the vineyards
	1525 - 1600	data acquisition of spread profile 2 (p-wave)
	1610 - 1700	data acquisition of spread profile 2 (s-wave)
	1700 - 1730	removal of the seismic measuring system
	1730	leaving from site

2.2 Summary of Data Acquisition Parameters

Compressional Wave Data Acquisition

# of active channels	96
geophone type	4.5 Hz natural frequency, vertical velocimeter
receiver station spacing	1.0 m
# of geophones/station	1
source point spacing	2.0 m to 3.0 m
source type	vertical hammer (8 kg) striking on a horizontal metal plate
sampling rate	500 µs
recording time	2048 ms
field filters	0.5 Hz LC, anti-alias
# of field records	45 (line 09SN_15STEIN-P1) and 46 (line 09SN_15STEIN-P2)

Shear Wave Data Acquisition

# of active channels	48
geophone type	10 Hz natural frequency, horizontal velocimeter
receiver station spacing	2.0 m
# of geophones/station	1
source point spacing	4.0 m to 6.0 m
source type	horizontal hammer (8 kg) striking horizontally at a metal-plated wooden beam anchored to the ground by means of 20 cm long spikes
sampling rate	500 µs
recording time	512 ms
field filters	2 Hz LC, anti-alias
# of field records	45 (line 09SN_15STEIN-S1) and 47 (line 09SN_15STEIN-S2)

Fig. 2.1: S-wave data acquisition at profile 09SN_15STEIN-2.

2.3 Composition of Seismic Field Crew

Personnel

Jochen Fiseli	Dipl.-Geologist, University of Freiburg i. Br., party chief
Dieter Martin	Dipl.-Geologist, University of Freiburg i. Br., party chief
Kieron Lynch	assistant, spread lay-out and activation of seismic source

Equipment

96	vertical geophones 4.5 Hz
48	horizontal geophones 12 Hz
6	seismic cables
1	seismic acquisition system Summit Compact, 96 channels
1	laptop computer for data acquisition
3	walkie-talkies
1	hammer 8 kg
1	steel plate
1	metal-plated wooden beam
1	van (FIAT Ducato 4x4)

2.4 Location

The seismic monitoring station STEIN (Stein am Rhein, SH) is situated in sediments of the Upper Freshwater Molasse (OSM, Miocene), bordered by elder glacio-fluviatile series of gravel sediments in the North and moraine sediments in the South.

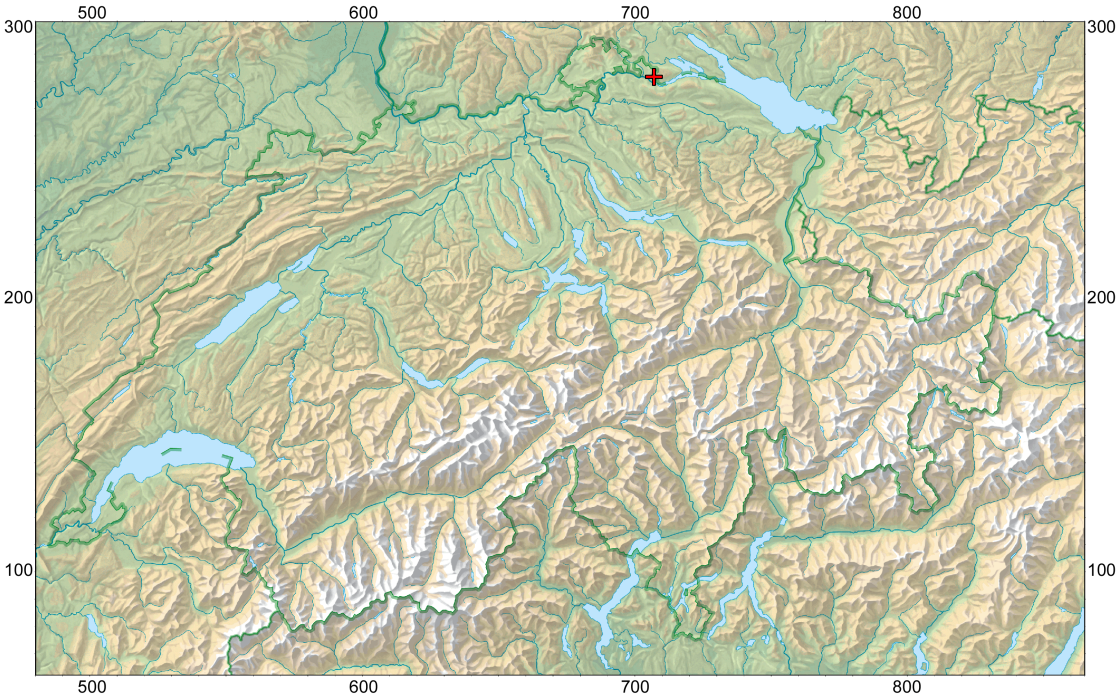

Fig. 2.2: The red cross marked seismic monitoring station STEIN (Stein am Rhein, SH) is located in Miocene deposits of the Upper Freshwater Molasse (OSM, Miocene). (map: geodata @ swisstopo).

2.5 Recording Conditions and Line Setup

Warm temperatures prevailed throughout the field data recording period.

Due to work in the vineyards,started in the afternoon, there was a lot of noise during the data acquisition period of profile 09SN_15STEIN-2. In general, the data quality obtained at STEIN is to be rated as good, except p-wave data of line 09SN_15STEIN-2.

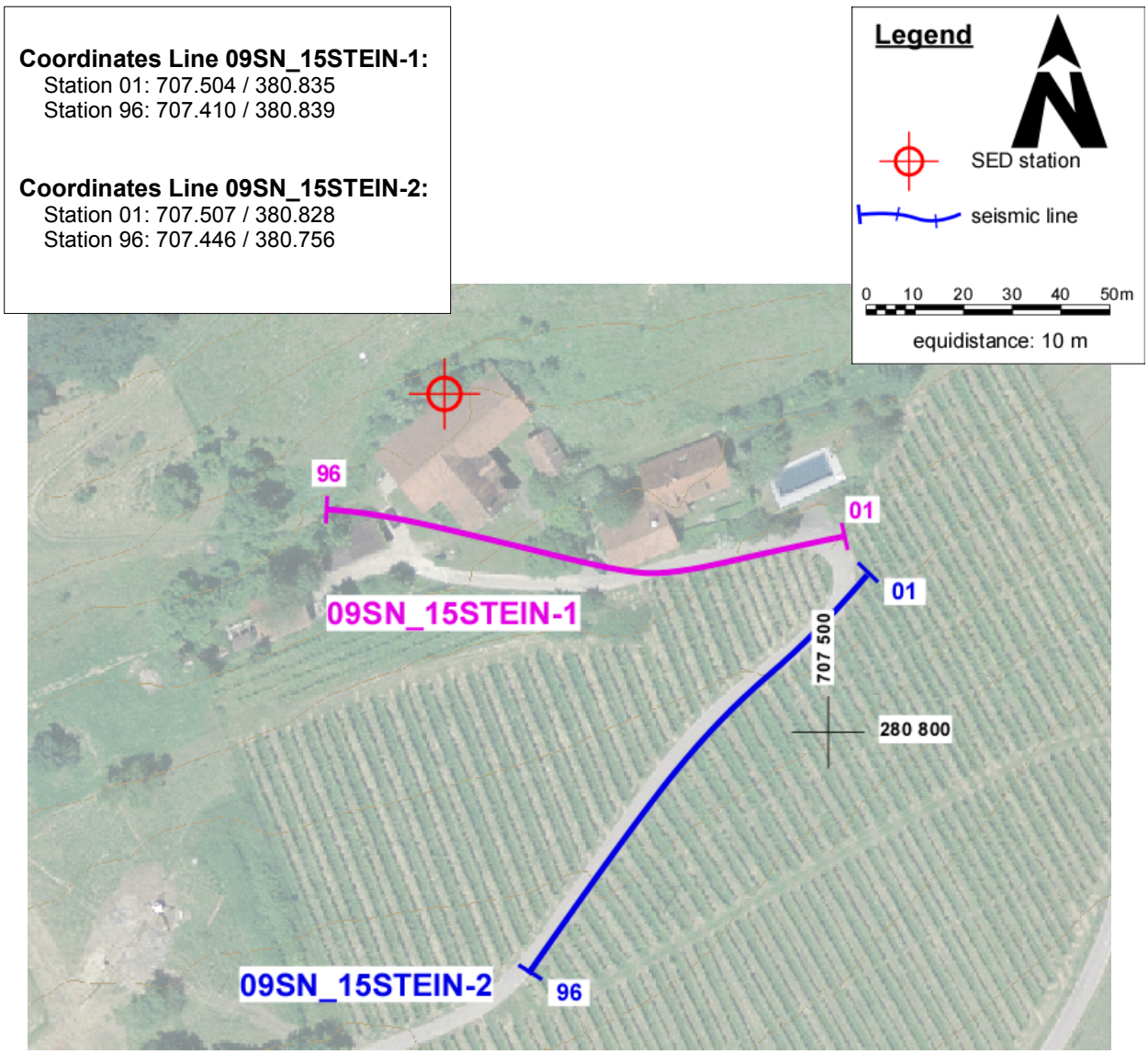

Fig. 2.3: Situation map with the trace of seismic profile 09SN_15STEIN-1 and -2. (background map: © GIS Kanton Schaffhausen)

3 SEISMIC DATA PROCESSING AND IMAGING OF THE RESULTS

3.1 General Remarks

- For the shear and compressional wave refraction seismic evaluation the package **RAYFRACT** by Intelligent Resources Ltd., Vancouver CAN, was used. The system features the technique of diving wave tomography (www.rayfract.com).
- The system **SPW** (**S**eismic **P**rocessing **W**orkshop) of Parallel Geoscience Corporation, Austin US-TX, was used for reflection seismic data processing (www.parallelgeo.com).
- Data processing of surface waves (MASW processing) was conducted with the software package **SurfSeis** V2.0 of Kansas Geological Survey in Lawrence US-KS.

A detailed description of the various surveying methods will be included in the general summary report.

3.2 Shear Wave Refraction Tomography

3.2.1 Reformatting and field geometry assignment

After reformatting the field data into the Rayfract format the field geometry is applied.

3.2.2 First break time picking

At each shot position, two seismic records were acquired in both activation directions. These two records are displayed superimposed with different colors on each other in Fig 3.2a together with the manually determined first arrival time picks.

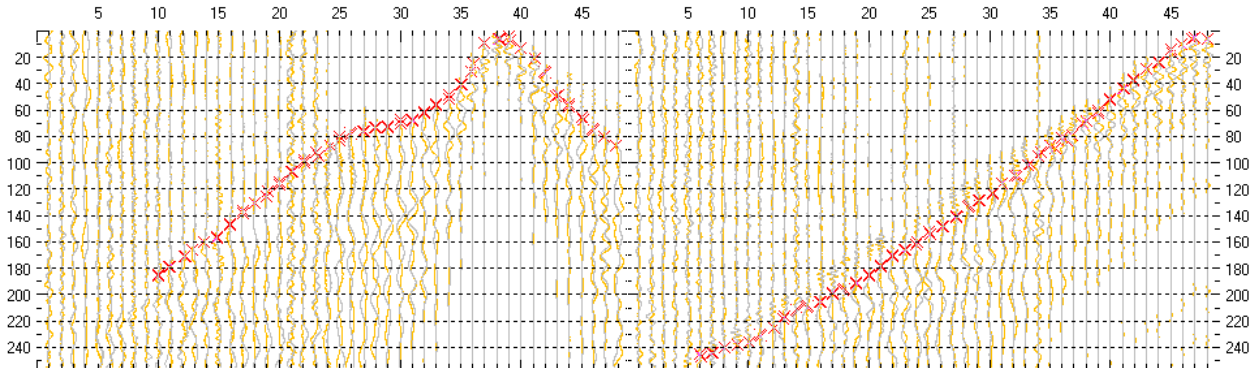

*Fig. 3.2a: High quality dual field record of line 09SN_15STEIN-S1 (left) and -S2 (right).showing at each station the s-wave traces with opposing polarities in different colors. The manually picked s-wave refraction arrivals at each station are marked with an **x**. The station spacing is 2 m, profile station number 00 = profile meter 0; profile station number 48 = profile meter 96.*

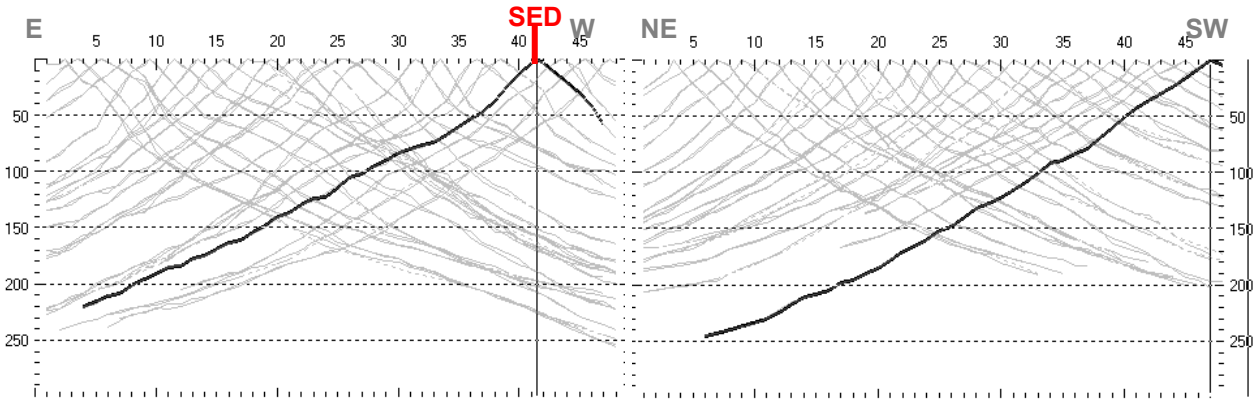

Fig. 3.2b: Curves of s-wave first break time picks of line 09SN_15STEIN-S1 (left) and -S2 (right).

3.2.3 Analytical Determination of Refraction Velocities

An initial 1D-velocity function (averaged 1D velocity-depth profiles derived by the Delta-t-V method, see Tab. 3.2a) is determined in the 3-dimensional time-offset-CMP-domain of all first break arrival time curves in the 3-dimensional time-offset-CMP-domain (see. Fig. 3.2c).

Depth [m]	Vs [m/s]
0.0	252
0.5	235
0.9	223
1.4	219
2.1	230
3.4	267
4.8	308
6.9	341
10.0	406
14.2	541
20.1	718
28.3	909
39.8	1220
55.8	1610

Depth [m]	Vs [m/s]
0.0	203
0.5	223
0.8	232
1.3	243
2.0	257
3.2	284
4.5	316
6.5	353
9.3	401
13.3	490
18.8	681
26.5	1038
37.4	1304

Tab. 3.2a: Initial 1D s-wave velocity function as mean values derived from real data of line 09SN_15STEIN-S1 (left) and -S2 (right).

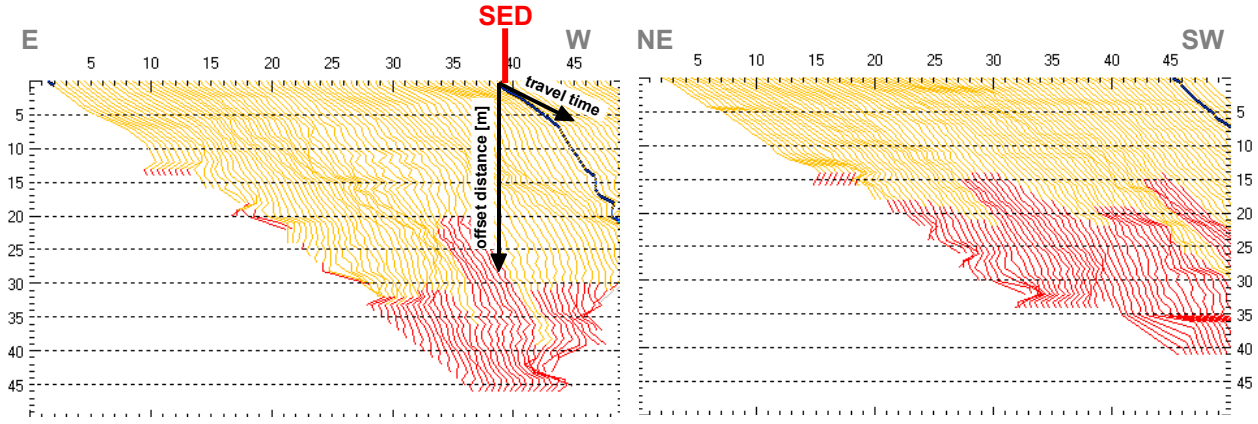

Fig. 3.2c: 3-dimensional distance-travel time diagrams of line 09SN_15STEIN-S1 (left) and -S2 (right) at the mid-points between source points and receiver stations are instrumental when using the analytical CMP derivation of the initial velocity field.
The horizontal axes are the along the CMP positions and the travel time respectively, the vertical axis denotes the offset distance between source and receiver positions. The colors represent different velocity layers. The station spacing is 2 m, profile station number 00 = profile meter 0; profile station number 48 = profile meter 96. The colors represent different velocity layers.

3.2.4 Tomographic inversion of the velocity gradient field by iterative modeling

The velocity field is iteratively refined by the subsequent Wavepath Eikonal Traveltime (WET) tomographic inversion process. The inversion results are portrayed in Fig. 3.2d as a gridded velocity contour section and in Fig. 3.2e as a ray path density section.

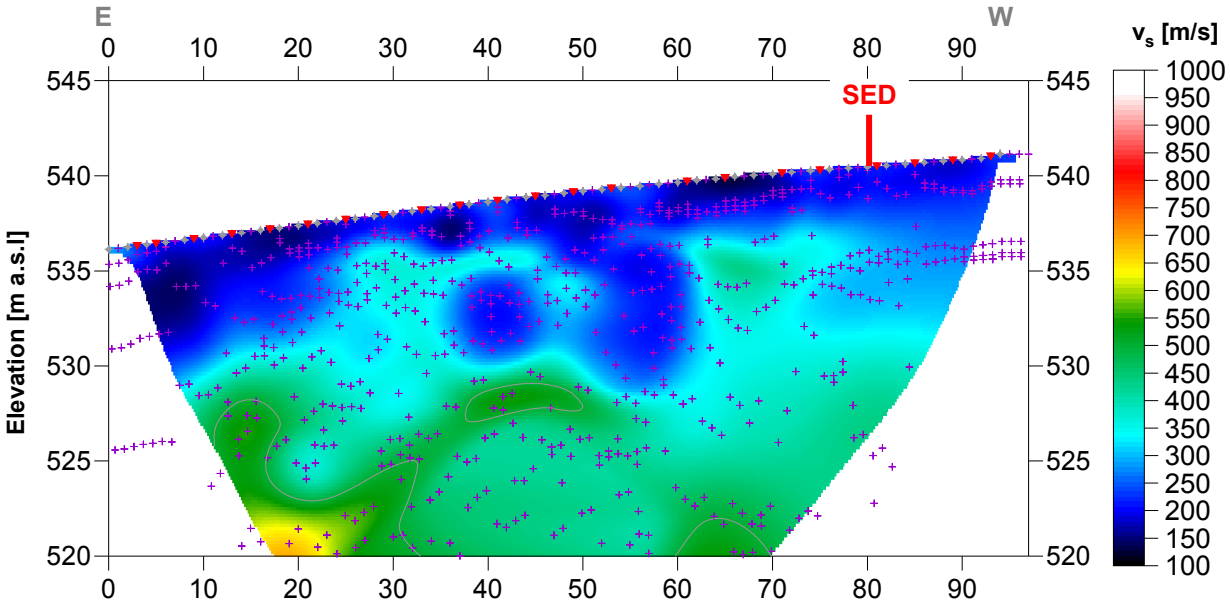

Fig. 3.2d: Shear wave velocity field of the line 09SN_15STEIN-S1. Red/white colors denote solid rock, blue/black colors point to unconsolidated sediments and soil.
Vertical axis: elevation [m a.s.l]; horizontal axis: profile meter; color encoded scale: v_s [m/s]; vertical exaggeration: 2:1; gray diamonds: receiver positions; red triangles: source positions; magenta crosses: positions of determined velocity values. The station spacing is 2 m, profile meter 0 = profile station number 00, profile meter 96 = profile station number 48.

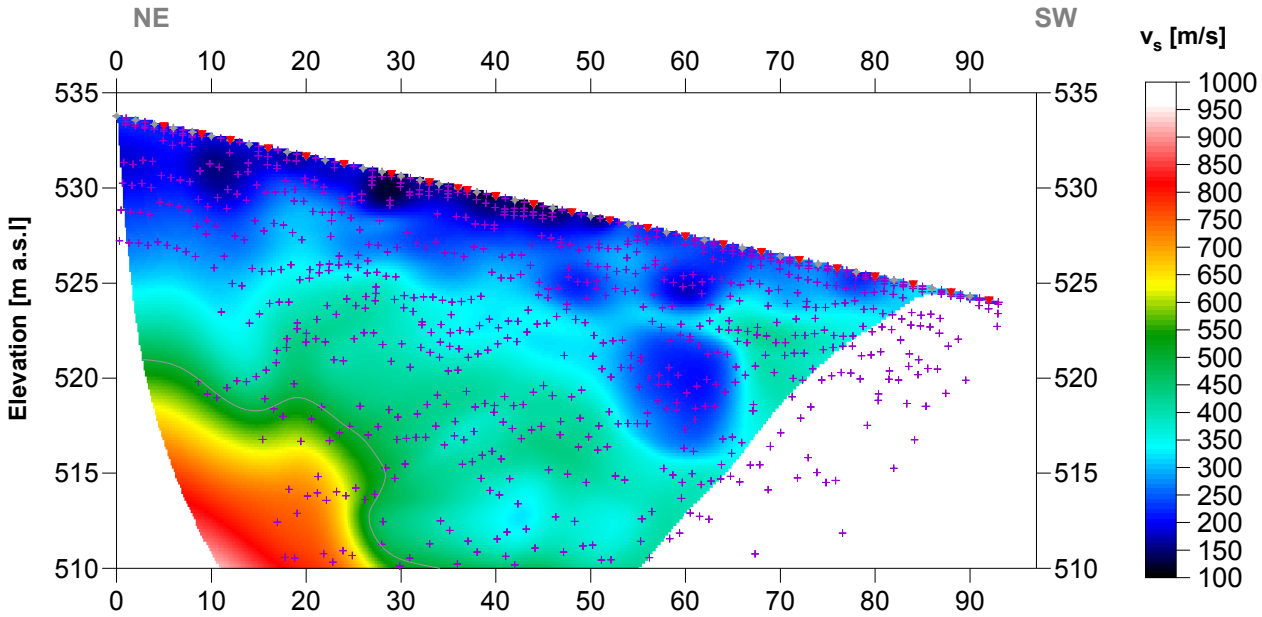

Fig. 3.2e: Shear wave velocity field of the line 09SN_15STEIN-S2. Red/white colors denote solid rock, blue/black colors point to unconsolidated sediments and soil.
Vertical axis: elevation [m a.s.l]; horizontal axis: profile meter; color encoded scale: v_s [m/s]; vertical exaggeration: 2:1; gray diamonds: receiver positions; red triangles: source positions; magenta crosses: positions of determined velocity values. The station spacing is 2 m, profile meter 0 = profile station number 00, profile meter 96 = profile station number 48.

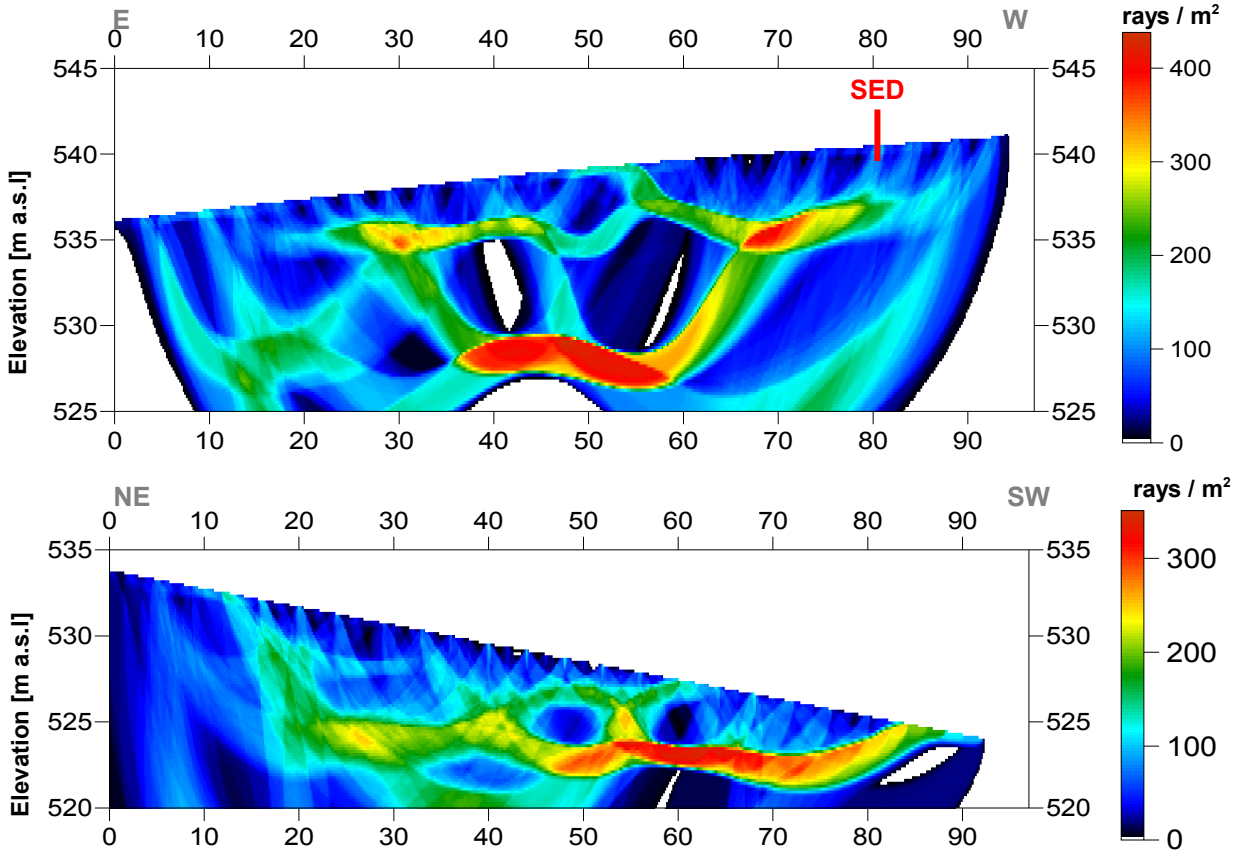

Fig. 3.2f: Shear wave ray path density along the seismic line 09SN_15STEIN-S1 (top) and -S2 (bottom). Red/white colors indicate high velocity contrasts (usually at the bedrock surface), blue/black colors denote low coverage areas. Vertical axis: elevation [m a.s.l]; horizontal axis: profile meter; color encoded scale: ray paths per m2; vertical exaggeration: 2:1. The station spacing is 2 m, profile meter 0 = profile station 00, profile meter 96 = profile station 48.

Depth [m]	Vs [m/s]
0.0	195
1.8	219
3.6	276
5.3	291
7.1	309
8.9	363
10.7	419
12.4	427
14.2	447
16.0	478
17.8	487
19.6	510
21.3	556
23.1	610
24.9	661
26.7	705

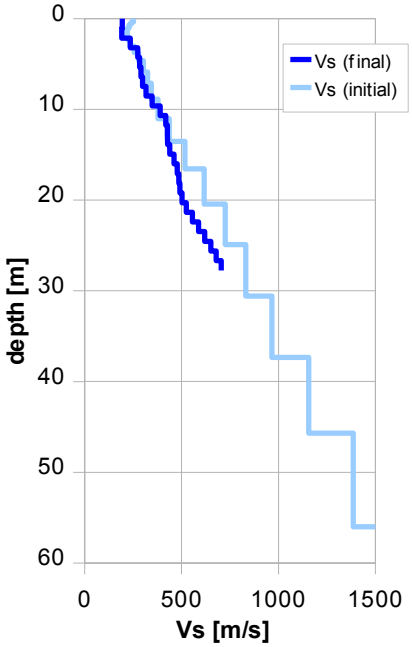

Tab. 3.2b: Final 1D s-wave velocity model derived from real data of line 09SN_15STEIN-S1 (horizontal average of all values) for the profile segment (between profile meters 5 and 45) with a geological setting resembling the one at the SED station. The calculated values of the initial 1D s-wave velocity model are given in Tab. 3.2a.

Depth [m]	Vs [m/s]
0.0	204
1.7	233
3.3	271
5.0	304
6.7	318
8.3	337
10.0	372
11.7	411
13.3	450
15.0	478
16.5	505
18.2	545
19.8	623
21.5	728
23.2	825
24.9	884

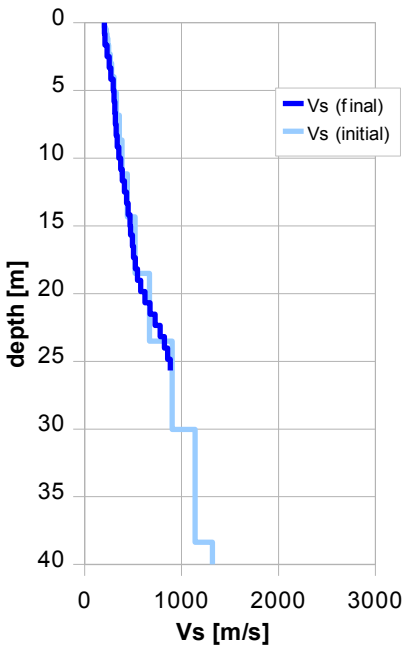

Tab. 3.2c: Final 1D s-wave velocity model derived from real data of line 09SN_15STEIN-S2 (horizontal average of all values) for the profile segment (between profile meters 30 and 50) with a geological setting resembling the one at the SED station. The calculated values of the initial 1D s-wave velocity model are given in Tab. 3.2a.

3.3 MASW Processing

3.3.1 Reformatting and field geometry assignment

The data preparation steps for the dispersion analysis include

- the assignment of the field acquisition geometry
- the selection of suitable offset ranges (=arrays) between 10 m and 50 m for dispersion, and the splitting of the field records in forward and reverse shooting direction data sets
- the reformatting of the data into the specific KGS format

X - - ... - - o-o-o-...-o-o-o (forward shooting or so-called PLUS direction)
respectively
o-o-o-...-o-o-o - - ... - - X (reverse shooting or so-called MINUS direction).

where **X** = shot position
o = receiver station
- = 1.0 m offset

The active array used at SED-station STEIN are the receiver station in the shot offset range between 10 and 50 m.

3.3.2 Calculating the dispersion image (overtone)

The result of dispersion analysis is the color encoded acoustic energy distribution in the phase velocity - frequency plane (see Fig. 3.3a and b).

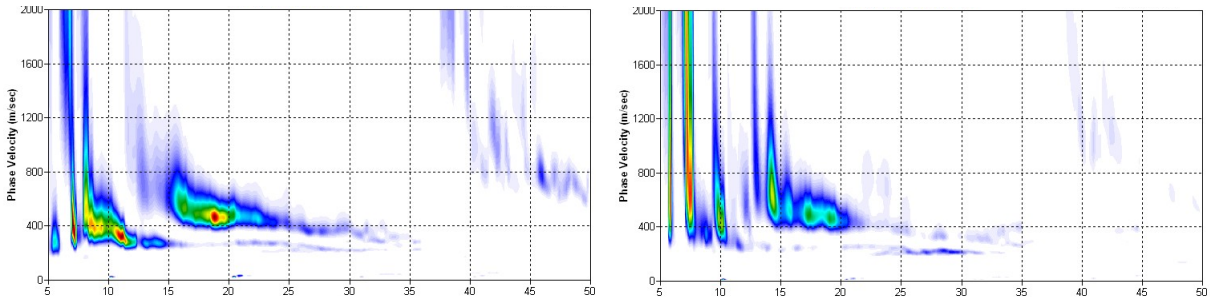

Fig. 3.3a: Dispersion image of high quality data (left) as found on 80 % and of fair quality data (right) representing about 20 % of the MASW dataset of site STEIN.
Horizontal axis: frequency from 5 to 50 Hz; vertical axis: phase velocity from 0 to 2000 m/s; color code: colors from white (no energy) to blue - green - yellow - red - black point to increasing energy amplitude values.

3.3.3 Analysis of the dispersion image

In the dispersion graphs as calculated in section 3.3.2 above, the curves joining the amplitude peaks of the fundamental modes are determined either by subjective inspection or in a semi-automated manner. On datasets with poorly defined amplitude peaks or with a highly irregular alignment of the peaks, the danger of obtaining improbable or wrong results is real and can only be mitigated by the processing experience and the a-priori knowledge of the geological setting by the geophysicist responsible for the data evaluation.

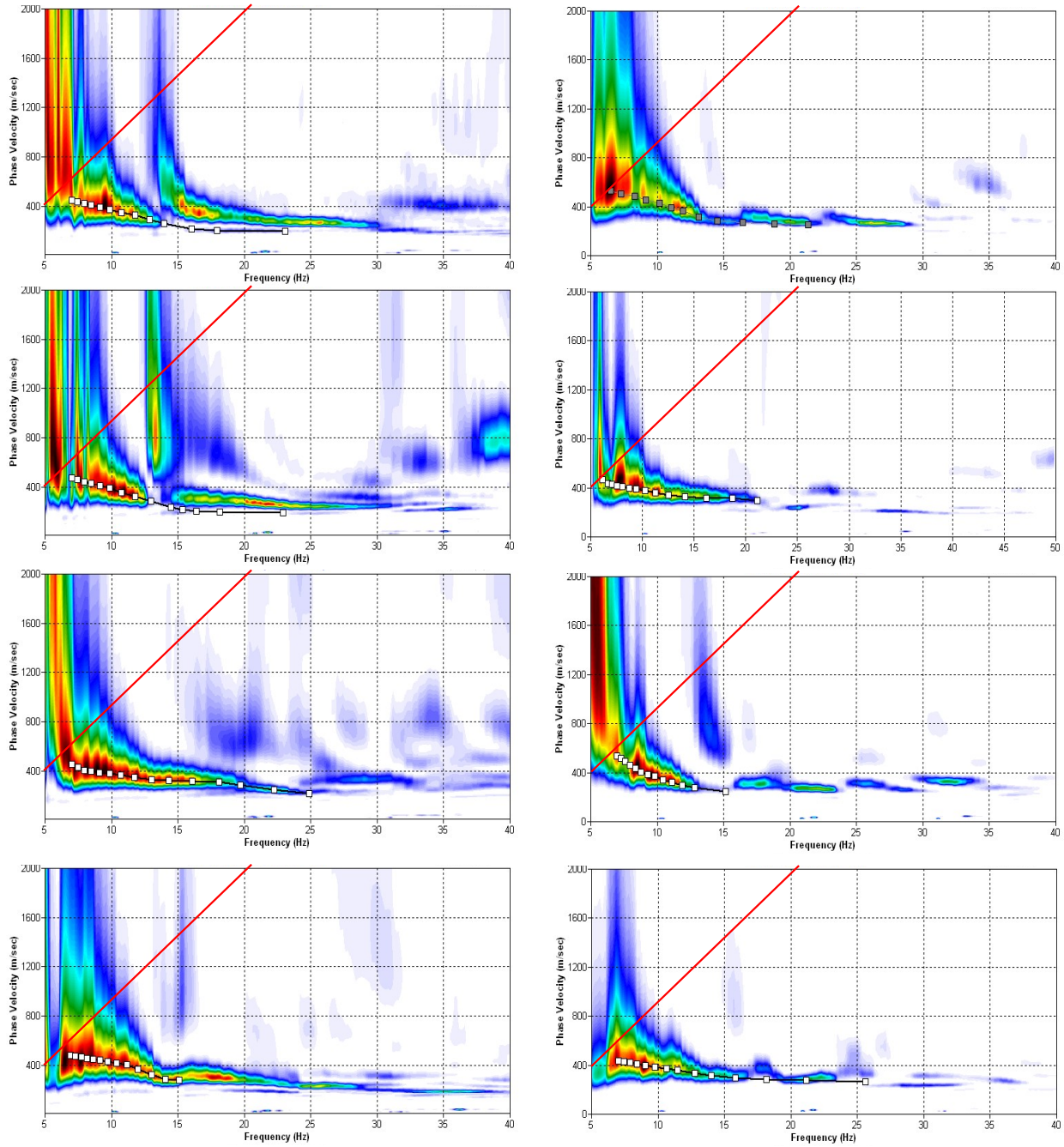

Fig. 3.3b: The manually picked dispersion images used for the derivation of the shear wave velocity section on line 09SN_15STEIN-M1. The dispersion curves (squares) are determined by linking the peaks of high energy. Note that 'higher modes' may at times produce higher energy peaks than the fundamental mode required for the analysis.
dotted fine line: signal-noise ratio for the designated f-v_{ph} – value.
red line: high resolution beam-forming curve for v_{max}.
1st row: left: station 31 @ PLUS direction; right: station 24 @ MINUS direction
2nd row: left: station 46 @ PLUS direction; right: station 45 @ MINUS direction
3rd row: left: station 61 @ PLUS direction; right: station 64 @ MINUS direction
4th row: left: station 76 @ PLUS direction; right: station 76 @ MINUS direction

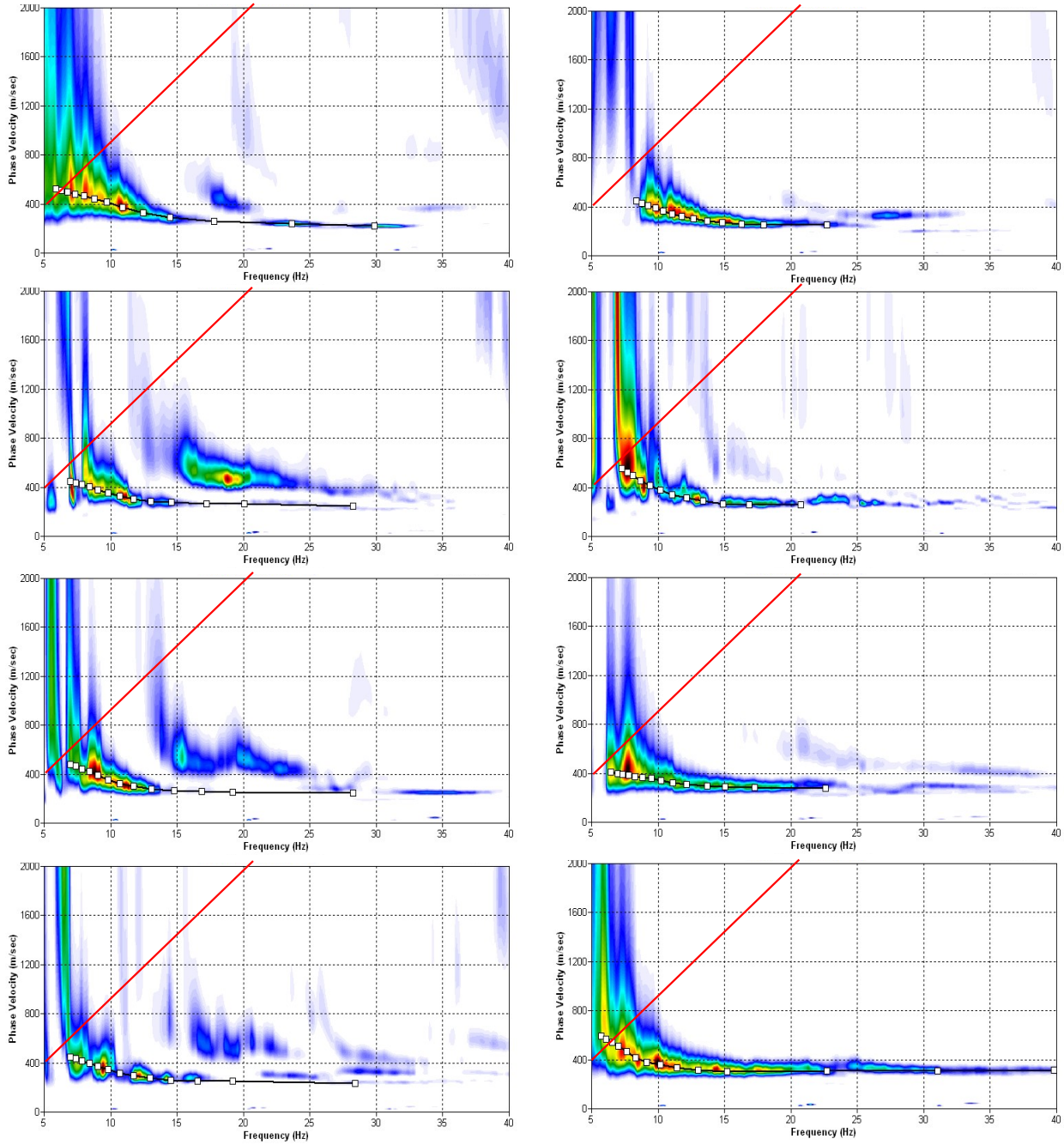

Fig. 3.3c: The manually picked dispersion images used for the derivation of the shear wave velocity section on line 09SN_15STEIN-M2. The dispersion curves (squares) are determined by linking the peaks of high energy. Note that 'higher modes' may at times produce higher energy peaks than the fundamental mode required for the analysis.
dotted fine line: signal-noise ratio for the designated f-v_{ph} – value.
red line: high resolution beam-forming curve for v_{max}.
1st row: left: station 30 @ PLUS direction; right: station 22 @ MINUS direction
2nd row: left: station 42 @ PLUS direction; right: station 42 @ MINUS direction
3rd row: left: station 57 @ PLUS direction; right: station 62 @ MINUS direction
4th row: left: station 75 @ PLUS direction; right: station 76 @ MINUS direction

3.3.4 Inversion of dispersion curves resulting in a 1D shear wave velocity distribution

Inversion of the extracted dispersion curves was performed using the algorithm described by Xia et al. (1999).

The inversion process is started by setting the maximum depth (z_{max}) to be in the order of 30% of the largest wavelength for an initial model consisting of 10 layers of increasing thicknesses. For all 10 layers the Poisson's ratio is assumed to be 0.4 and the rock/soil density to be 2.0 g/cm^3. The inversion process is concluded either after twelve iterations or when the convergence condition of a RMS-error of less than 3 m/s (phase velocity) is met.

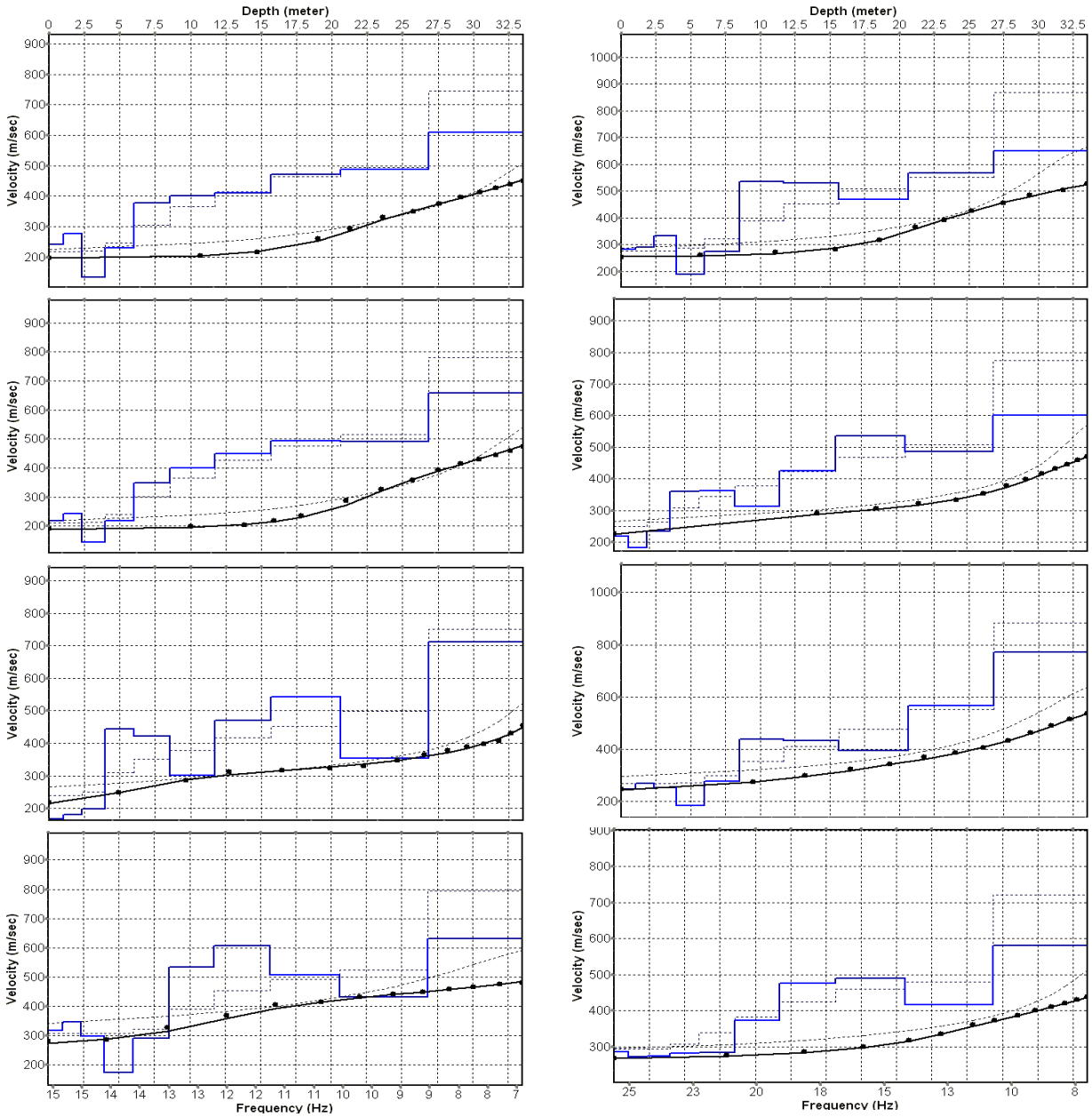

Fig. 3.3d: Inversion results of dispersion curves of dataset at line 09SN_15STEIN-M1.
***brown**: Inversion of dispersion curve (dots) resp. of the modeled dispersion curve (dotted line: initial model; continuous line: end model). Horizontal axis: frequency Hz, vertical axis: v_s.*
***blue**: 10-layer-model (dotted: initial model, continuous line: final model). Horizontal axis: depth, vertical axis: phase velocity resp. v_S).*
1st row: left: station 31 @ PLUS direction; right: station 24 @ MINUS direction
2nd row: left: station 46 @ PLUS direction; right: station 45 @ MINUS direction
3rd row: left: station 61 @ PLUS direction; right: station 64 @ MINUS direction
4th row: left: station 76 @ PLUS direction; right: station 76 @ MINUS direction

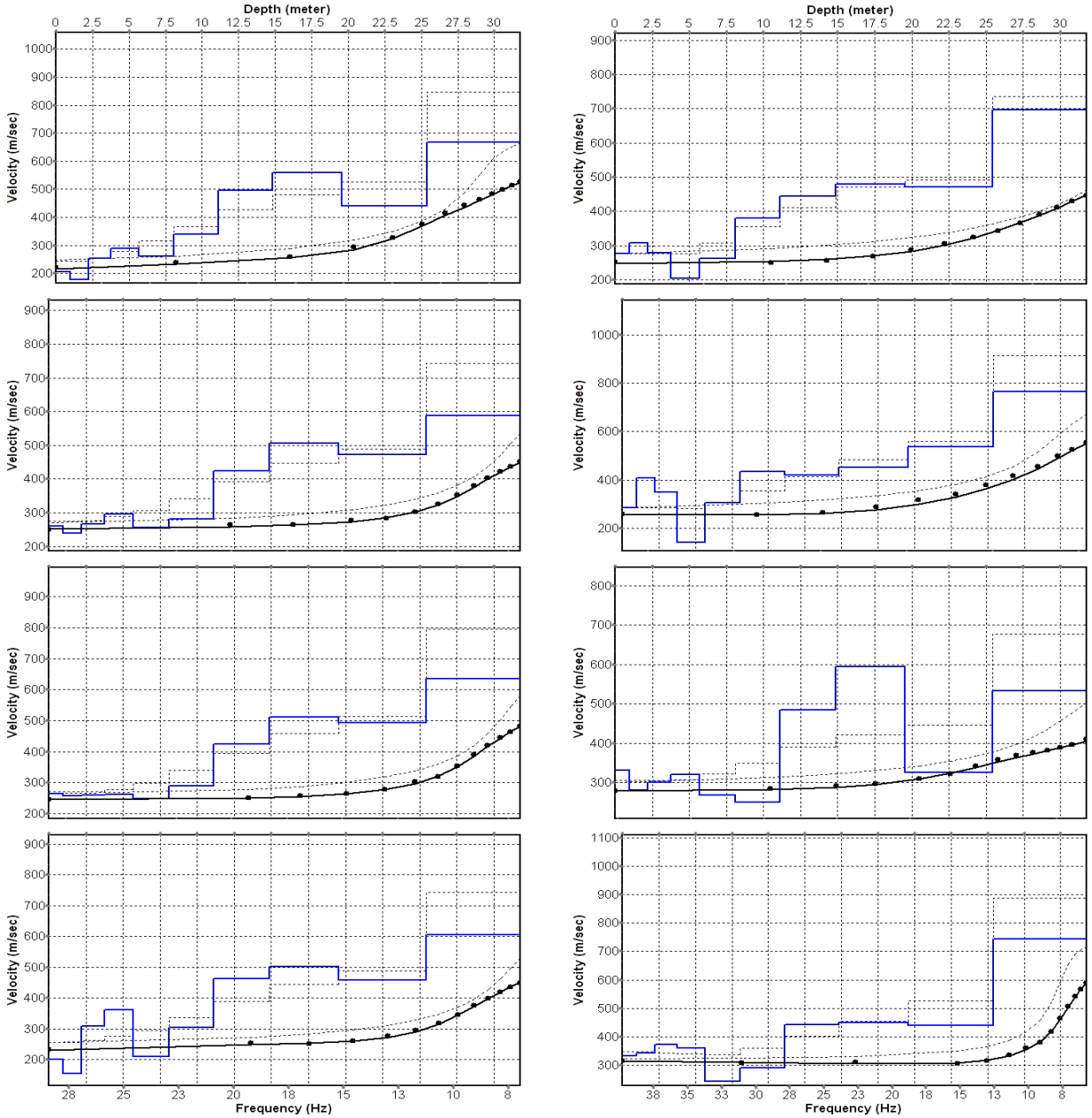

Fig. 3.3e: Inversion results of dispersion curves of dataset at line 09SN_15STEIN-M2.
***brown**: Inversion of dispersion curve (dots) resp. of the modeled dispersion curve (dotted line: initial model; continuous line: end model). Horizontal axis: frequency Hz, vertical axis: v_s.*
***blue**: 10-layer-model (dotted: initial model, continuous line: final model). Horizontal axis: depth, vertical axis: phase velocity resp. v_S).*
1st row: left: station 30 @ PLUS direction; right: station 24 @ MINUS direction
2nd row: left: station 42 @ PLUS direction; right: station 42 @ MINUS direction
3rd row: left: station 57 @ PLUS direction; right: station 62 @ MINUS direction
4th row: left: station 75 @ PLUS direction; right: station 76 @ MINUS direction

Dispersion analyses of records with longer receiver arrays should – by theory – increase the investigation depth. At STEIN, with both lines and both directions, MASW processing with the maximal array length of 96 m doesn't improve the results (Fig. 3.3f and 3.3g).

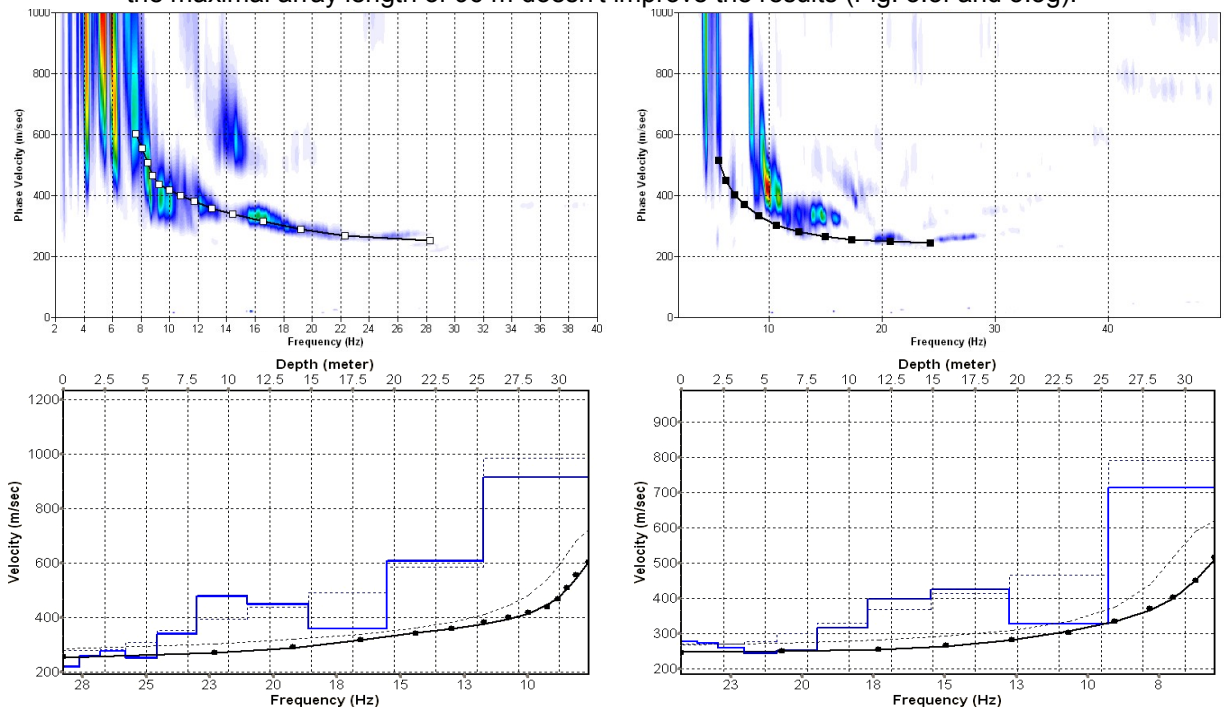

Fig. 3.3f: Top: dispersion images of over-all arrays (10...106 m offset) of line 09SN_15STEIN-M1 in PLUS (left) and MINUS (right) direction; dotted fine line: signal-noise ratio for the designated f-v_{ph}-value. Red line: high resolution beam-forming curve for v_{max}.
*Below: The two respective inversion results; **brown**: inversion of dispersion curve; **blue**: 10-layer-model. Horizontal axis: depth, vertical axis: phase velocity resp. v_s.*

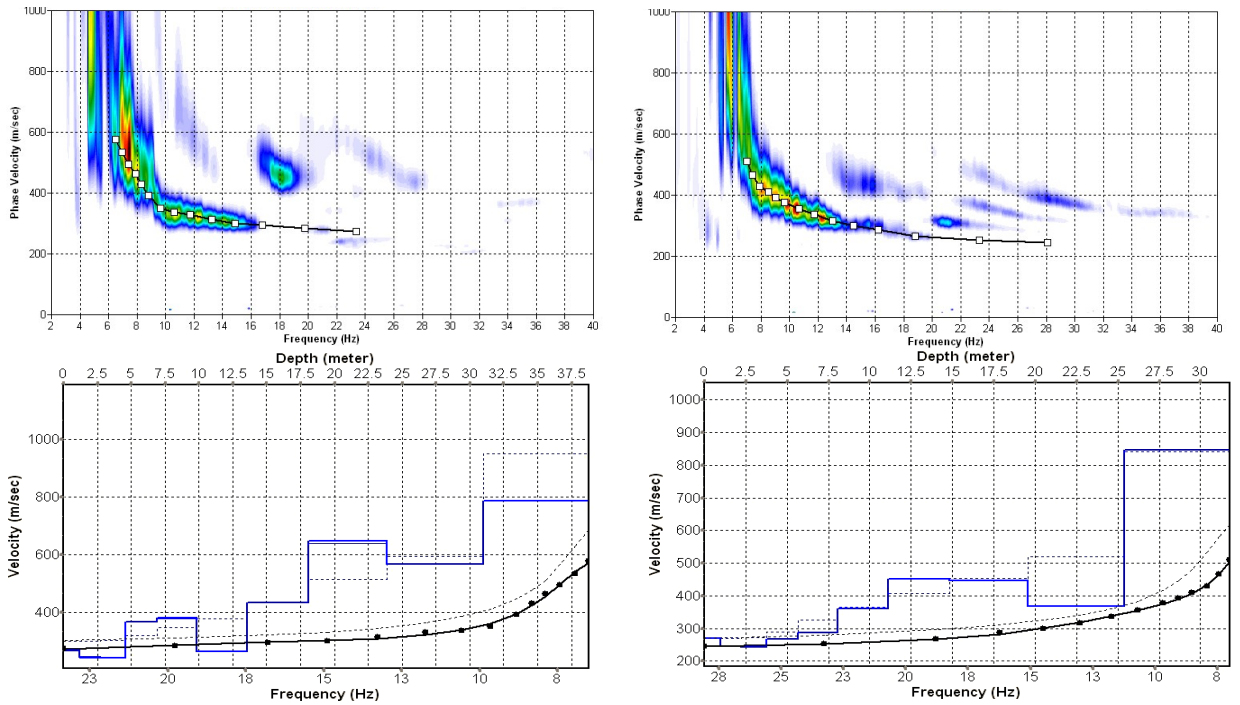

Fig. 3.3g: Top: dispersion images of over-all arrays (10...106 m offset) of line 09SN_15STEIN-M2 in PLUS (left) and MINUS (right) direction; dotted fine line: signal-noise ratio for the designated f-v_{ph} – value. Red line: high resolution beam-forming curve for v_{max}.
*Below: The two respective inversion results; **brown**: inversion of dispersion curve; **blue**: 10-layer-model. Horizontal axis: depth, vertical axis: phase velocity resp. v_s.*

3.3.5 Gridding and plotting of 2D v_s-velocity field

By assembling the 1D v_s - depth functions of all stations the final 2D v_s-field is derived using a Kriging gridding procedure as portrayed in Fig. 3.3h and 3.3i below:

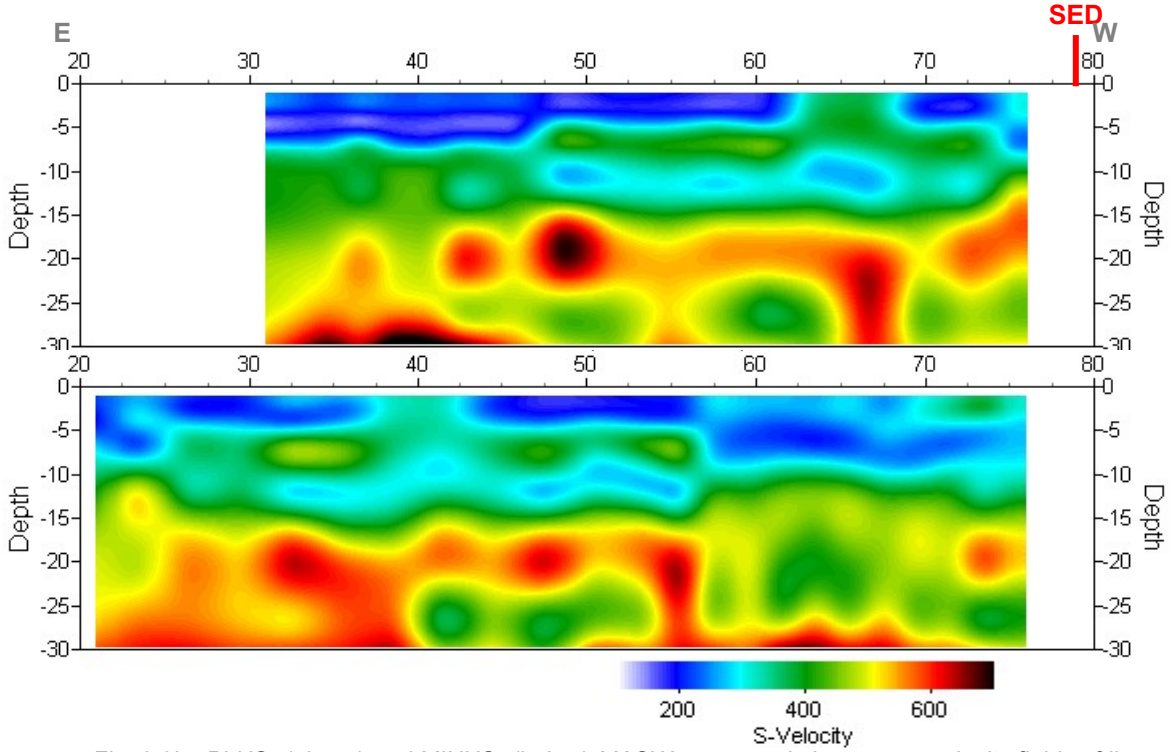

Fig. 3.3h: PLUS- (above) and MINUS- (below)-MASW-processed shear wave velocity fields of line 09SN_15STEIN-M1. Station spacing is 1 m.

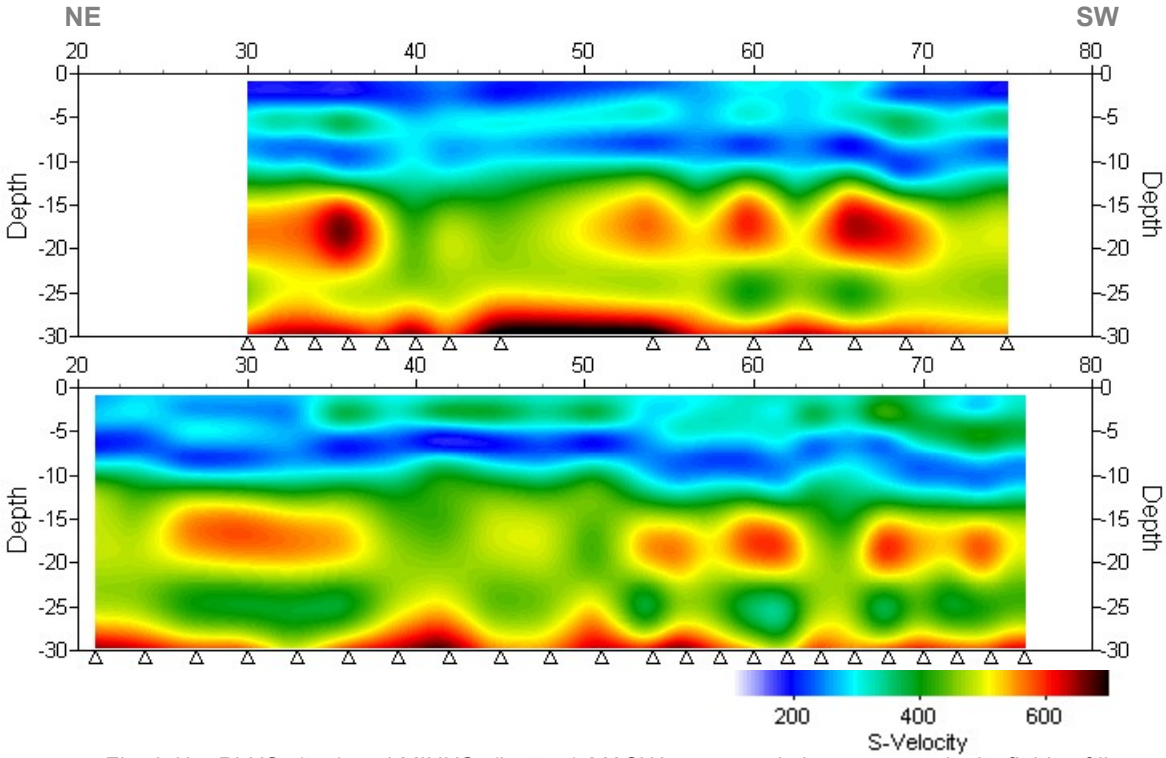

Fig. 3.3i: PLUS- (top) and MINUS- (bottom)-MASW-processed shear wave velocity fields of line 09SN_15STEIN-M2. Station spacing is 1 m.

3.3.6 Calculation of the average shear wave velocity

In order to calculate a representative shear wave velocity-depth function of line 09SN_15STEIN-M1 at the SED station, all computed 1D-v_s-depth functions are averaged (non-weighted mean values). The v_s-depth-function is shown in Tab. 3.3a.

Depth [m]	Vs+ [m/s]	Vs- [m/s]	Vs [m/s]
0.0	263	239	251
1.0	257	229	243
2.3	259	224	241
4.0	302	323	313
6.0	321	359	340
8.5	350	346	348
11.7	462	470	466
15.7	526	549	538
20.6	486	488	487
26.8	713	703	708

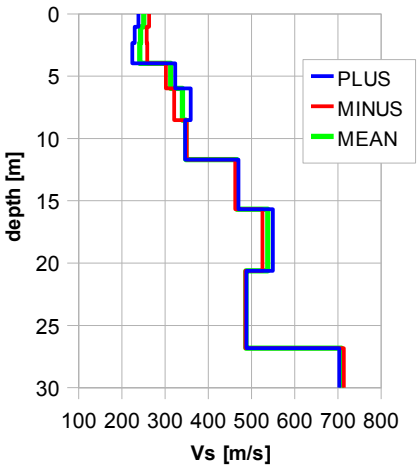

Tab. 3.3a: Averaged vs - depth function of line 09SN_15STEIN-M1 at the SED station STEIN. Blue line: MASW-'PLUS' processing, red line: MASW-'MINUS' processing; green line: average of PLUS- and MINUS-functions.

In order to calculate an representative shear wave velocity-depth function of line 09SN_15STEIN-M2 at the SED station, all computed 1D-v_s-depth functions between seismic profile station are averaged (non-weighted mean values). The resulting v_s-depth-function is shown in Tab. 3.3b.

Depth [m]	Vs- [m/s]	Vs+ [m/s]	Vs [m/s]
0.0	302	241	272
1.0	320	214	267
2.2	331	277	304
3.8	265	315	290
5.7	245	246	246
8.1	336	303	320
11.1	475	481	478
14.9	516	541	528
19.5	430	470	450
25.4	670	699	684

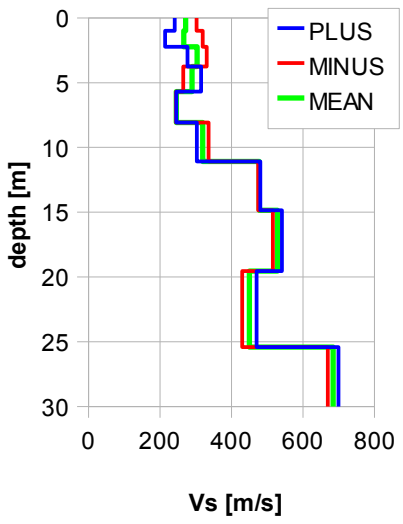

Tab. 3.3b: Averaged v_s - depth function of line 09SN_15STEIN-M2 at the SED station STEIN. Blue line: MASW-'PLUS' processing, red line: MASW-'MINUS' processing; green line: average of PLUS- and MINUS-functions.

The inversion of the four 100 m-array dispersion curves data (10 to 106 m offset, see Fig. 3.3f and 3.3g) are given in Tab. 3.3c. These values are complemented with the values derived of the 40 m-arrays analyses (Tab. 3.3a and 3.3b).

100 m array								40 m array			
depth	m1+	m1-	m2+	m2-	m1	m2	m	depth	m1	m2	m
1.0	217	276	265	268	247	267	253	0.0	251	272	261
2.3	259	273	243	246	266	245	259	1.0	243	267	255
4.0	277	259	242	244	268	243	259	2.3	241	304	273
6.0	251	244	367	267	247	317	287	4.0	313	290	301
8.5	339	253	380	286	296	333	324	6.0	340	246	293
11.7	479	315	264	360	397	312	353	8.5	348	320	334
15.7	449	399	434	452	424	443	427	11.7	466	478	472
20.6	357	426	646	446	391	546	476	15.7	538	528	533
26.8	610	327	566	367	469	467	501	20.6	487	450	469
33.5	915	714	786	847	814	817	805	26.8	708	684	696

Tab. 3.3c: v_S-depth values of the four MASW-derived dispersion curves of both seismic line 09SN_15STEIN-M1 and 09SN_15STEIN-M2 using 100 m-arrays. The dispersion curves are shown in Fig. 3.3f and Fig 3.3g.

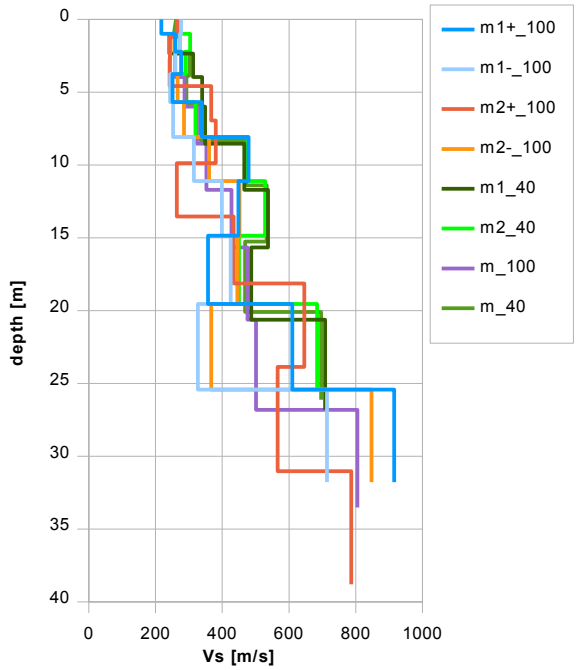

Fig. 3.3j: Comparison of the ensemble of inversion results of both lines 09SN_15STEIN-M1 and -M2, either using the 40 m- and the 100 m-arrays.
blue lines: analyses of records of line 09SN_15STEIN-M1
red lines: analyses of records of line 09SN_15STEIN-M2
magenta line: mean of both 100 m-array records analyses in MINUS and PLUS direction.
green lines: v_S-values of analyses of 40 m-array records.

3.3.7 Calculation of the shear wave velocity scalars $v_{s,5}$, $v_{s,10}$, ...

The parameters $v_{s,5}$, $v_{s,10}$, $v_{s,20}$, $v_{s,30}$, $v_{s,40}$, $v_{s,50}$ represent the average shear wave velocities in the depth interval between the surface and the respective depth levels and are determined from the formula

$$v_{s,n} = \frac{\sum_{i=1}^{n} d_i}{\sum_{i=1}^{n} d_i / v_{si}}$$

with:

d_i = thickness of layer i

v_{si} = corresponding shear-wave velocity.

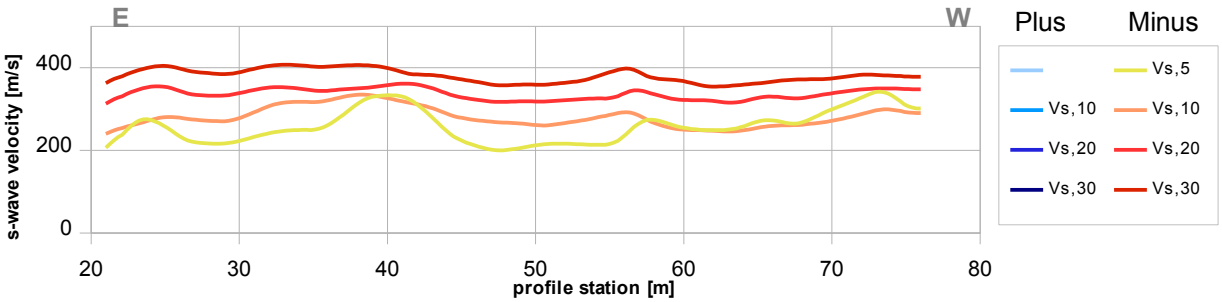

Fig. 3.3k: Graphs of the averaged vs,5...-values along the line 09SN_15STEIN-M1 for the PLUS- (blue lines) and MINUS- (red lines) directions.

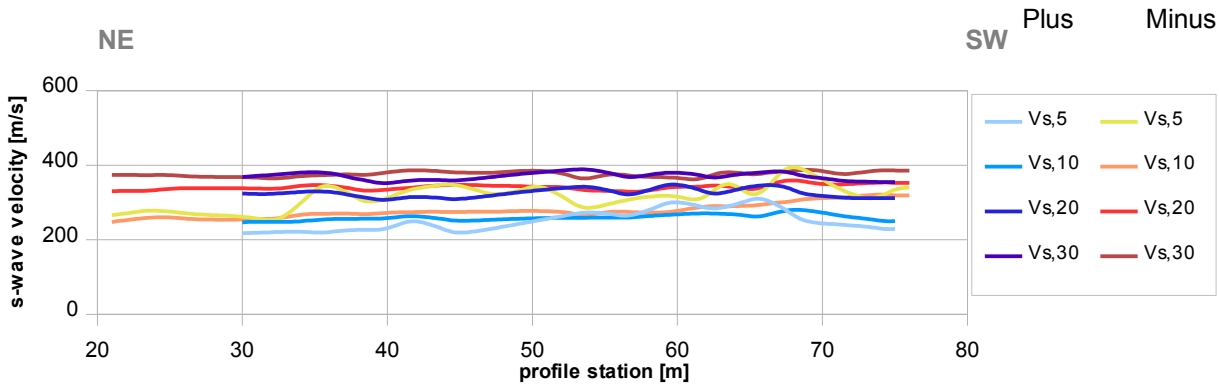

Fig. 3.3l: Graphs of the averaged $v_{s,5}$...-values along the line 09SN_15STEIN-M2 for the PLUS- (blue lines) and MINUS- (red lines) directions.

The average values of the s-wave velocity model $v_{s,5}$, $v_{s,10}$, $v_{s,20}$, $v_{s,30}$, $v_{s,40}$, $v_{s,50}$, $v_{s,100}$ (= average shear wave velocity from the surface to depths of 5 m, …until 100 m) on the line segment nearest to the SED station (Tab. 3.3d) are summarized below:

	Vs,5	Vs,10	Vs,20	Vs,30	Vs,40	Vs,50
MINUS	259	281	336	381	n/a	n/a
PLUS	231	272	330	376	n/a	n/a
MEAN	245	277	333	378	n/a	n/a

	Vs,5	Vs,10	Vs,20	Vs,30	Vs,40	Vs,50
MINUS	315	278	341	376	n/a	n/a
PLUS	252	260	326	371	n/a	n/a
MEAN	283	269	333	373	n/a	n/a

Tab. 3.3d: The average shear wave velocities within the depth intervals from surface down to 5 m, etc. … to 50 m, calculated as mean values from all inversion results; line 09SN_15STEIN-M1, top; line 09SN_15STEIN-M2, bottom).

3.4 Hybrid Seismic Data Processing

3.4.1 p-wave *Reflection* Seismic Processing Sequence

A) Data conditioning

A1 Reformatting and quality verification of field data
A2 Recording geometry assignment
A3 Data editing (suppression of bad / dead traces, etc.)
A4 Preliminary analysis of refraction velocities

B Filtering and deconvolution

B1 Analytical muting of refraction arrivals
B2 Amplitude recovery / amplitude equalization in time and frequency domains
B3 Predictive deconvolution parameter tests / application
B4 Determination of band limiting corner frequencies / application
B5 Optional 2-D filtering

C) Velocity analysis and stack

C1 Common Depth Point (CDP) sort
C2 Semblance velocity analysis using supergathers of 3 - 5 CDP's
C3 Optional dip move-out correction
C4 Normal Move-Out (NMO) correction and application of stretch mute
C5 Band-pass filtering
C6 CDP stack
C7 Optional coherency filtering

D) Time-depth conversion

D1 Optional spiking deconvolution
D2 Band-pass filtering
D3 Depth conversion
D4 Final display of seismic depth section with inversed polarity (non-SEG-convention)

3.4.2 The presentation of reflection seismic data

The data in a reflection seismic section are presented as an assembly of individual seismic signals at regular intervals along a seismic profile. The simplest way of representing the signals are single wiggle lines (first to the left in the illustration below). A more capturing presentation is the variable area form (second to the left). Combining these two modes results in the var-wiggle mode. Another method of data visualization is the variable density mode (second from the right).

The compressional phase of seismic signals is defined in this report as the onset of the positive amplitude excursion in black (Fig. 3.4a). Since the source signal is produced by an explosion or by an impact at the surface, the signal starts off with a compression of the ground particles. Thus the arrivals of reflection events are defined by the compressional phase.

In rare situations of velocity inversions, cases in which formation velocities are lower than in the layers above, polarity reversals of the reflected signals occur. The beginning of the reflection event would then be characterized by a dilatational phase, represented in this report as a negative amplitude excursion, i.e. in white.

The final p-wave seismic depth sections are displayed in Fig. 3.4b and 3.4c, the hybrid sections in Fig. 3.4j and -k further below.

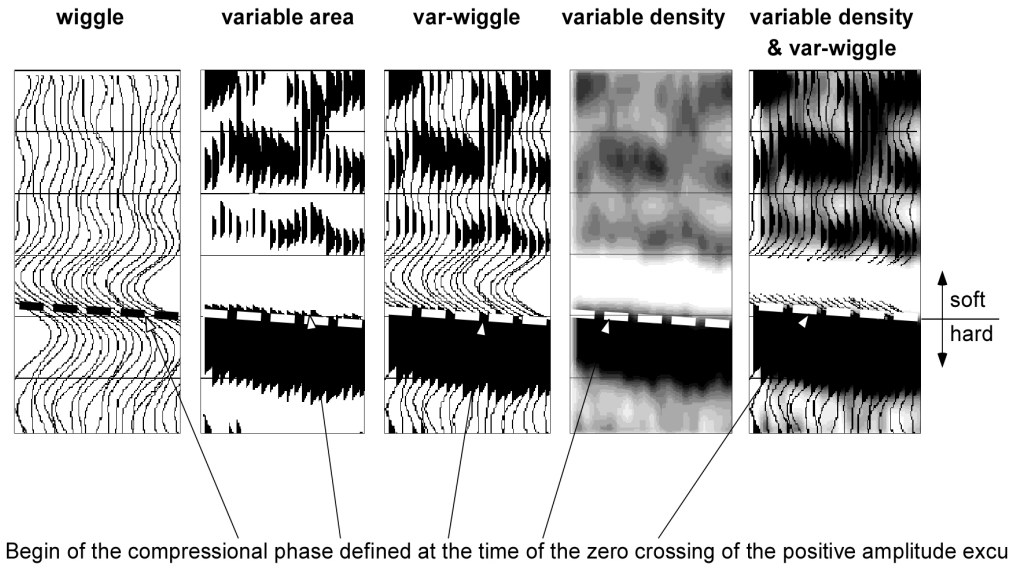

Fig. 3.4a Representation of reflection seismic data and the definition of a reflection event.

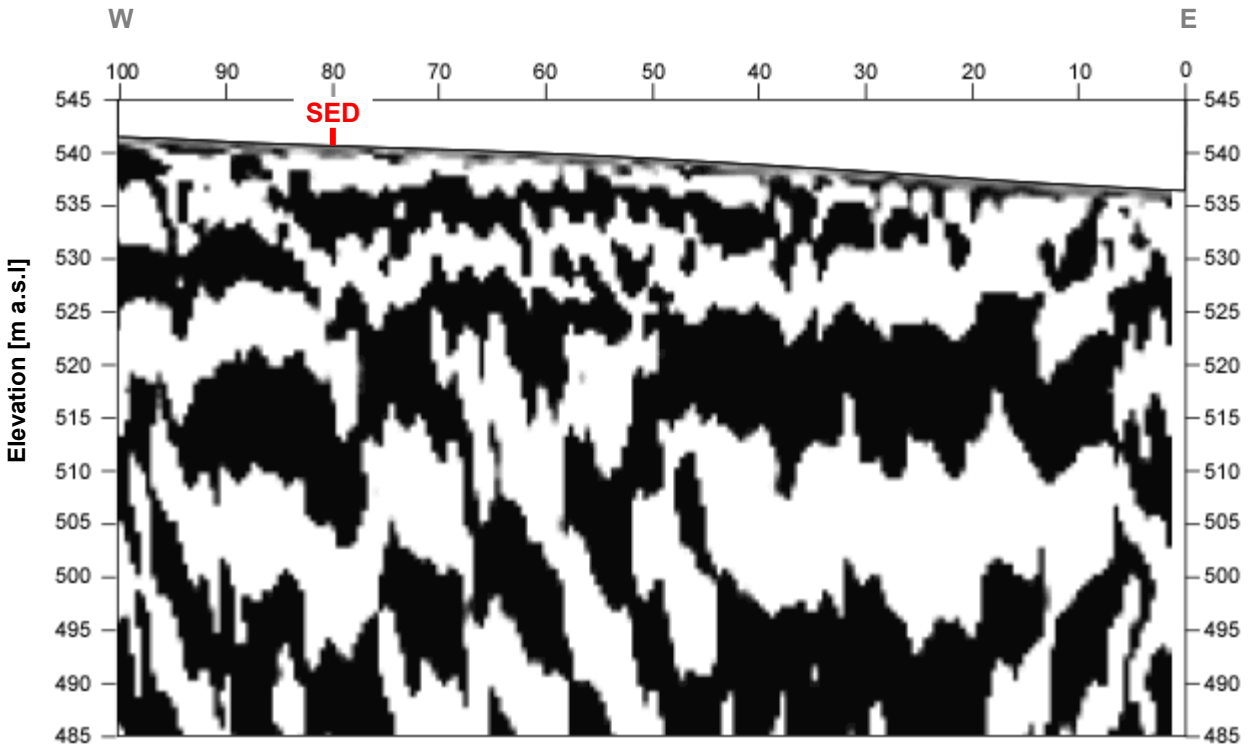

Fig. 3.4b: Seismic depth section of seismic line 09SN_15STEIN-P1 with variable density mode presentation. Vertical axis: elevation [m a.s.l.], horizontal axis: profile meter; no vertical exaggeration. The station spacing is 1 m.

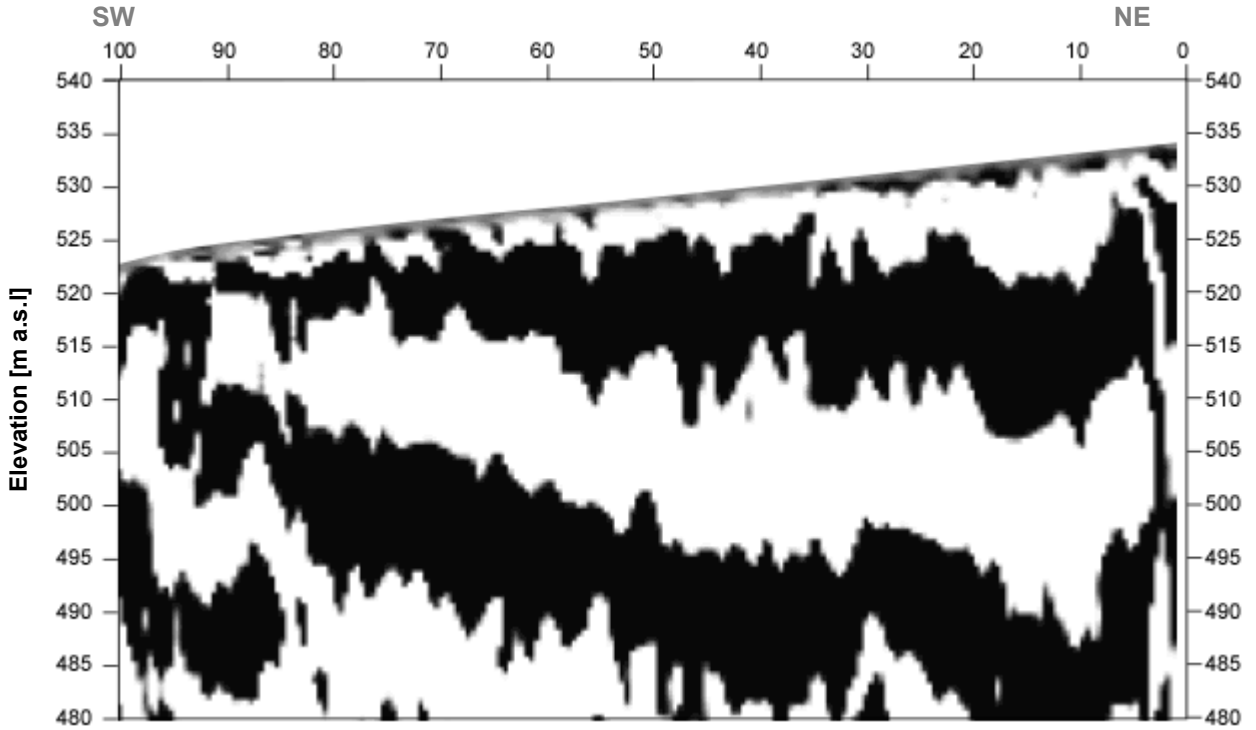

Fig. 3.4c: Seismic depth section of seismic line 09SN_15STEIN-P2 with variable density mode presentation. Vertical axis: elevation [m a.s.l.], horizontal axis: profile meter; no vertical exaggeration. The station spacing is 1 m.

3.4.3 p-wave refraction tomography processing

The seismic p-wave refraction processing steps are analogous to those described in paragraph 3.2. For a detailed method statement and a description of the processing steps please refer to the summary report. The Figs. 3.4d to 3.4i and Tab. 3.4a illustrate the intermediate processing steps and the final result.

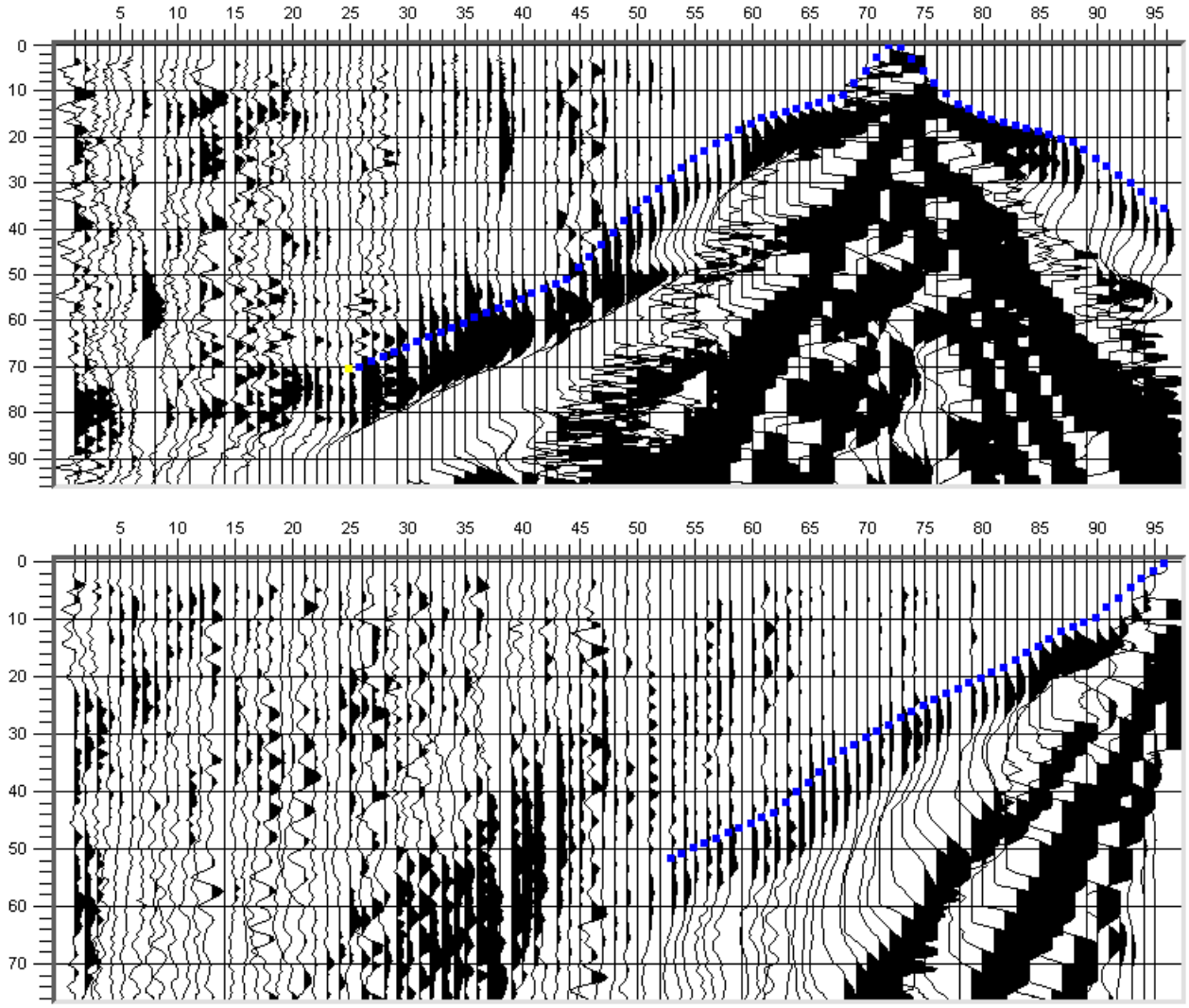

Fig. 3.4d: p-wave records of 09SN_15STEIN-P1 (above) and -P2 (below) with positive amplitude excursions in black. Blue squares mark the manually picked first break arrival times. Vertical axis: travel time in ms, horizontal axis: station numbers spaced at 1 m.

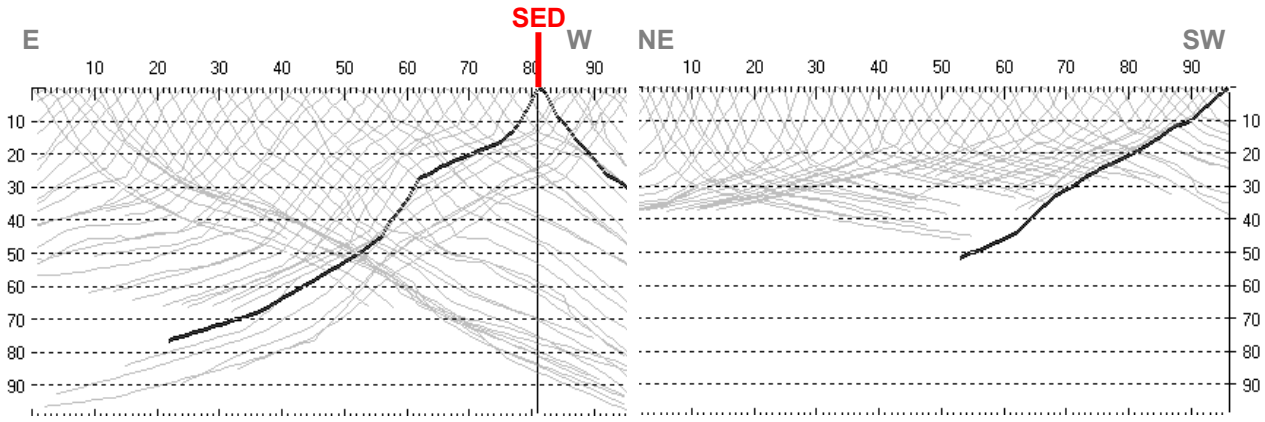

Fig. 3.4e: Travel time curves of p-wave arrival time picks of line 09SN_15STEIN-P1 (left) and -P2 (right). Vertical axes: travel time [ms], horizontal axes: station number (= profile meter).

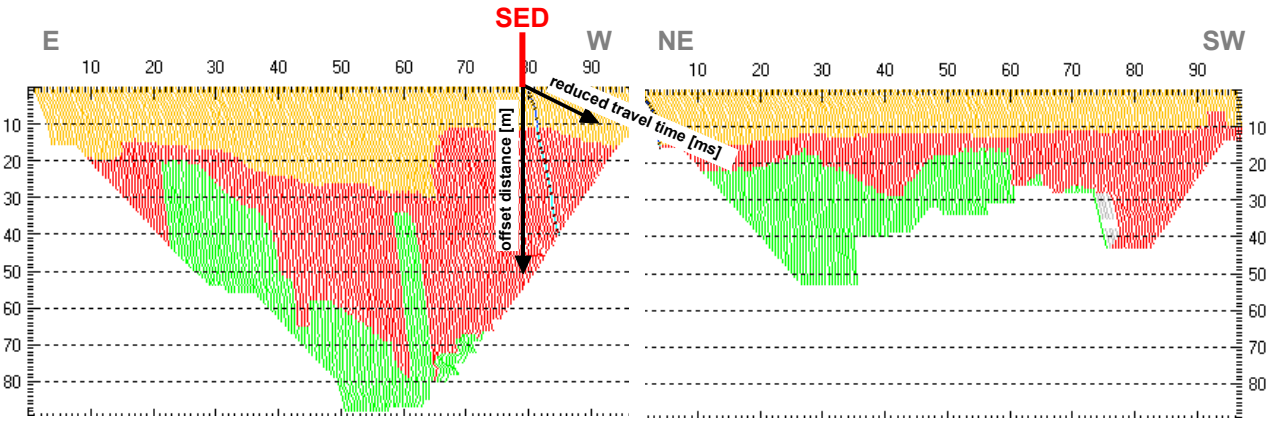

Fig. 3.4f: 3-dimensional distance-travel time diagrams at the mid-points between source points and receiver stations are instrumental when using the analytical CMP derivation of the initial velocity field. The horizontal axes are along the CMP positions and the travel time respectively, the vertical axis denotes the offset distance between source and receiver positions.

Depth [m]	Vp [m/s]
0.0	522
0.2	500
0.5	451
1.2	477
1.7	540
2.4	630
3.2	708
4.4	749
5.9	827
8.0	1020
10.5	1272
13.9	1533
18.3	1821
23.9	2181
31.3	2880
41.0	3706
53.3	4390

Depth [m]	Vp [m/s]
0.0	410
0.1	412
0.4	398
0.6	416
0.9	428
1.2	451
1.7	552
2.3	660
3.2	844
4.2	1068
5.7	1336
7.5	1652
9.8	1851
12.9	2121
16.8	3249
22.1	2728

Tab. 3.4a: Initial 1D p-wave velocity model derived from real data (left: 09SN_15STEIN-P1; right: -P2).

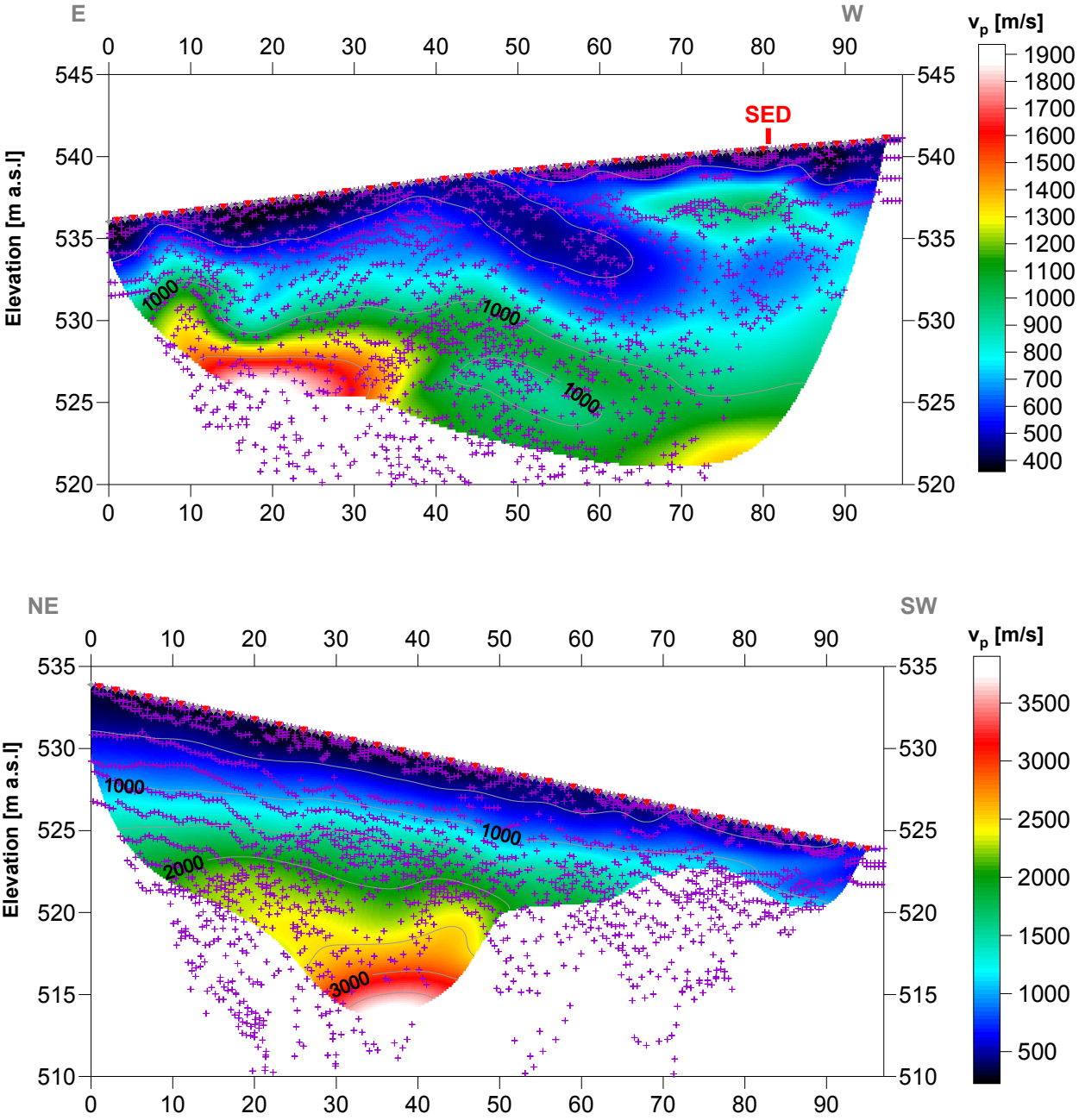

Fig. 3.4g: Compressional wave velocity field image along the seismic profiles 09SN-15STEIN-P1 (above) and -P2 (below). Red/white colors indicate solid rock, blue/black colors unconsolidated sediments and soil. Vertical axis: elevation [m a.s.l]; horizontal axis: profile meter; color scale: v_s [m/s]; vertical exaggeration: 2:1; gray squares: receiver stations; red triangles: shot positions; magenta crosses: positions of determined velocity values.

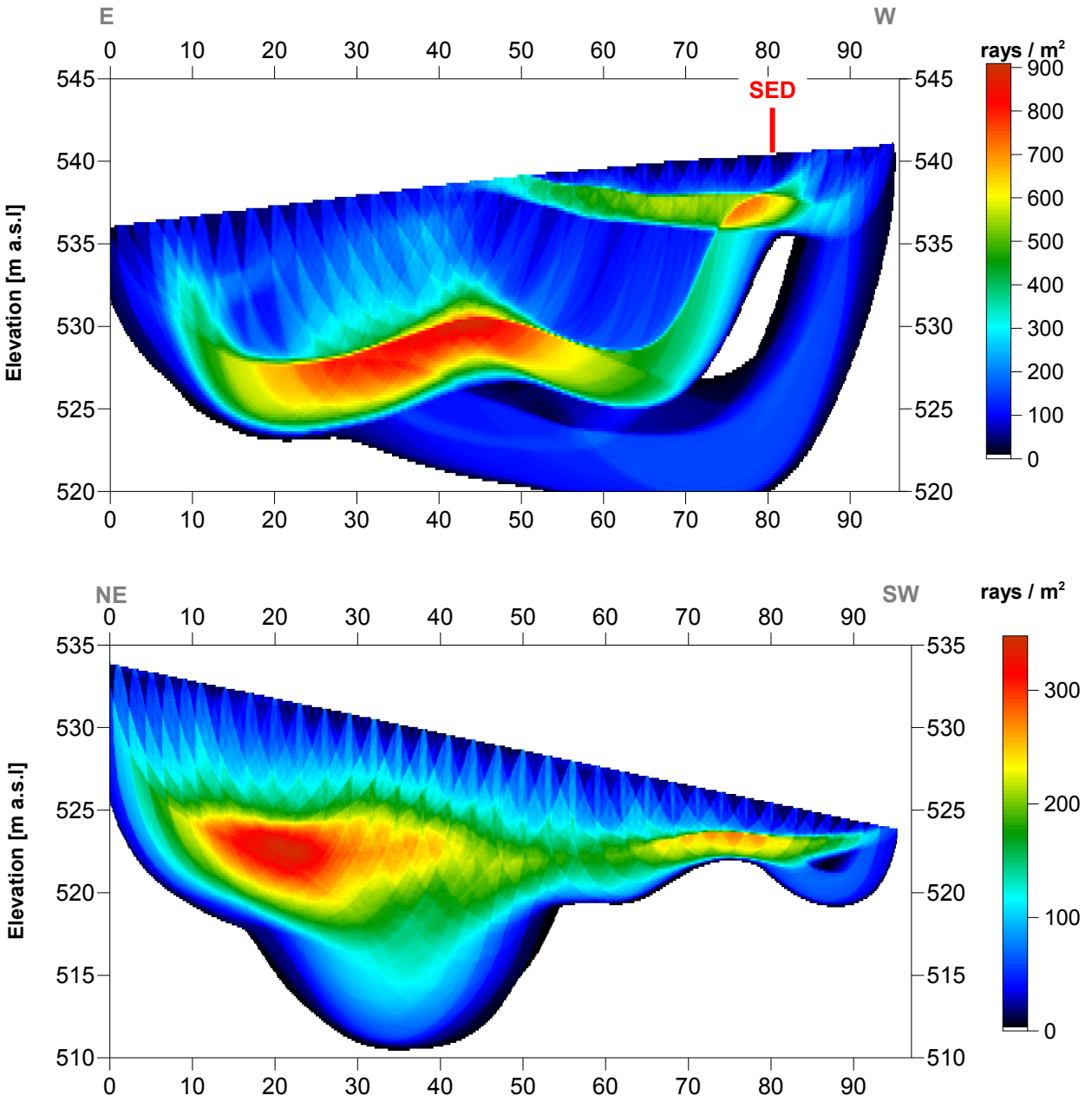

Fig. 3.4h Compressional wave subsurface ray path density along the seismic profiles 09SN_15STEIN-P1 (above) and -P2 (below). Red/white colors indicate high velocity contrast between two layers, blue/black colors low coverage areas. Vertical axis: elevation [m a.s.l]; horizontal axis: profile meter; color scale: ray paths per m2; vertical exaggeration: 2:1.

Depth [m]	Vp [m/s]
0.0	427
1.2	480
2.2	585
3.2	673
4.2	715
5.2	731
6.3	756
7.3	812
8.3	902
9.3	1002
10.3	1103
11.3	1129
12.4	1063
13.4	1009
14.4	1017
15.4	1040
16.4	1090
17.4	1169
18.5	1255

Depth [m]	Vp [m/s]
0.0	374
1.0	433
2.0	597
2.9	786
3.9	972
4.9	1195
5.9	1424
6.9	1642
7.9	1828
8.8	2015
9.8	2170
10.8	2307
11.8	2454
12.8	2617
13.8	2852
14.7	3125
15.7	3451

Tab. 3.4b: Final 1D p-wave velocity model as horizontal mean values of line 09SN_15STEIN-P1 (left) line -P2 (right) .

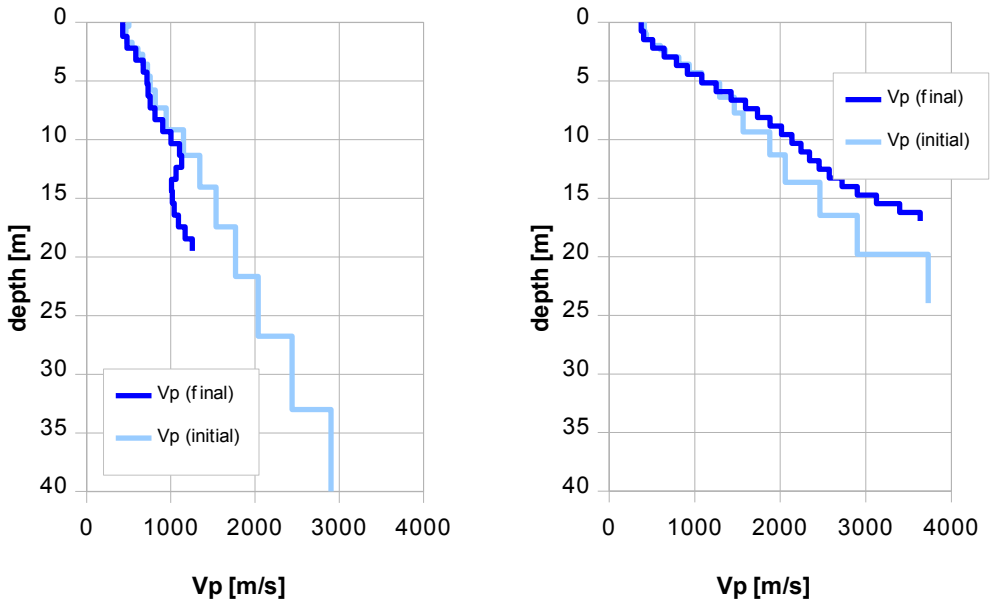

Fig. 3.4i: Final 1D p-wave velocity model as horizontal mean values of line 09SN_15STEIN-P1 (left) resp. line -P2 (right). Initial 1D p-wave velocity model values are given in Tab. 3.4a.

3.4.4 Representation of the hybrid seismic section

The hybrid seismic section is the reflection seismic section with the superimposed p-wave velocity field. It portrays the geological structures and the p-wave velocity field, the latter being indicative for the rock / soil rigidity. The uninterpreted hybrid seismic section is portrayed in Fig. 3.4j and 3.4k below.

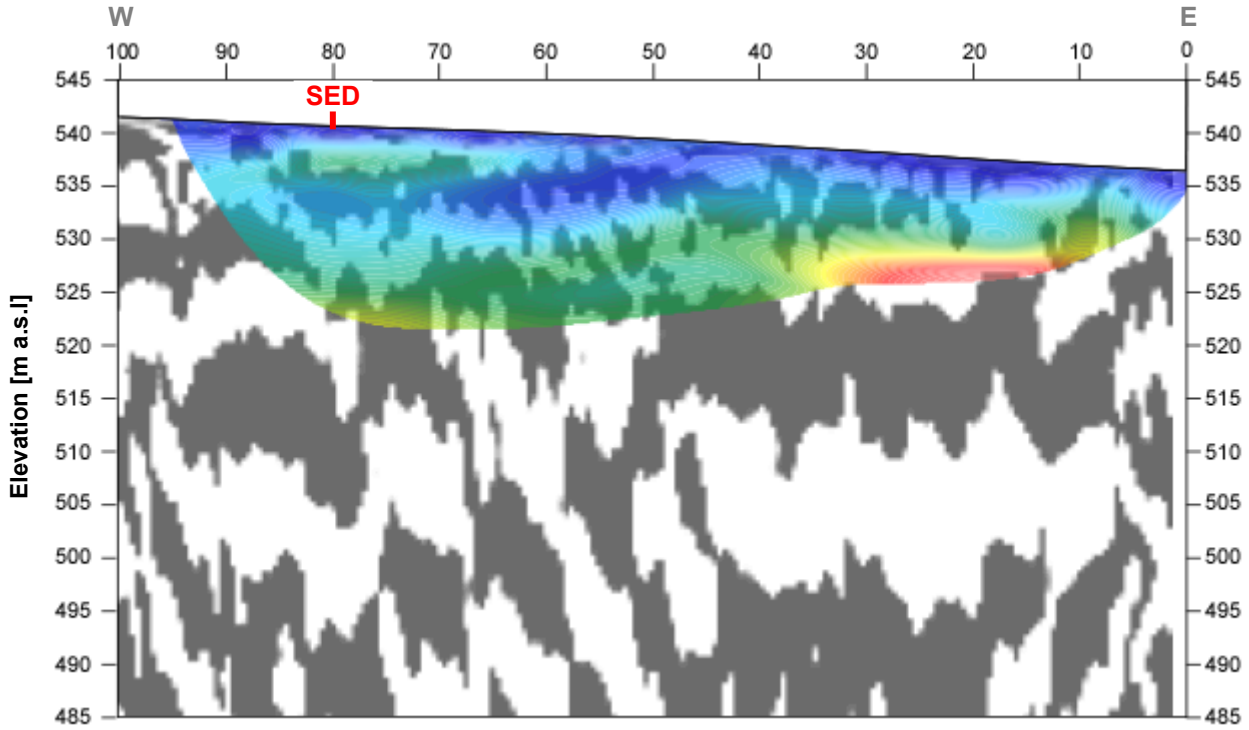

Fig. 3.4j Uninterpreted hybrid seismic section 09SN_15STEIN-P1: superimposed onto the seismic reflection section is the color encoded p-velocity field derived by refraction tomography (no vertical exaggeration).

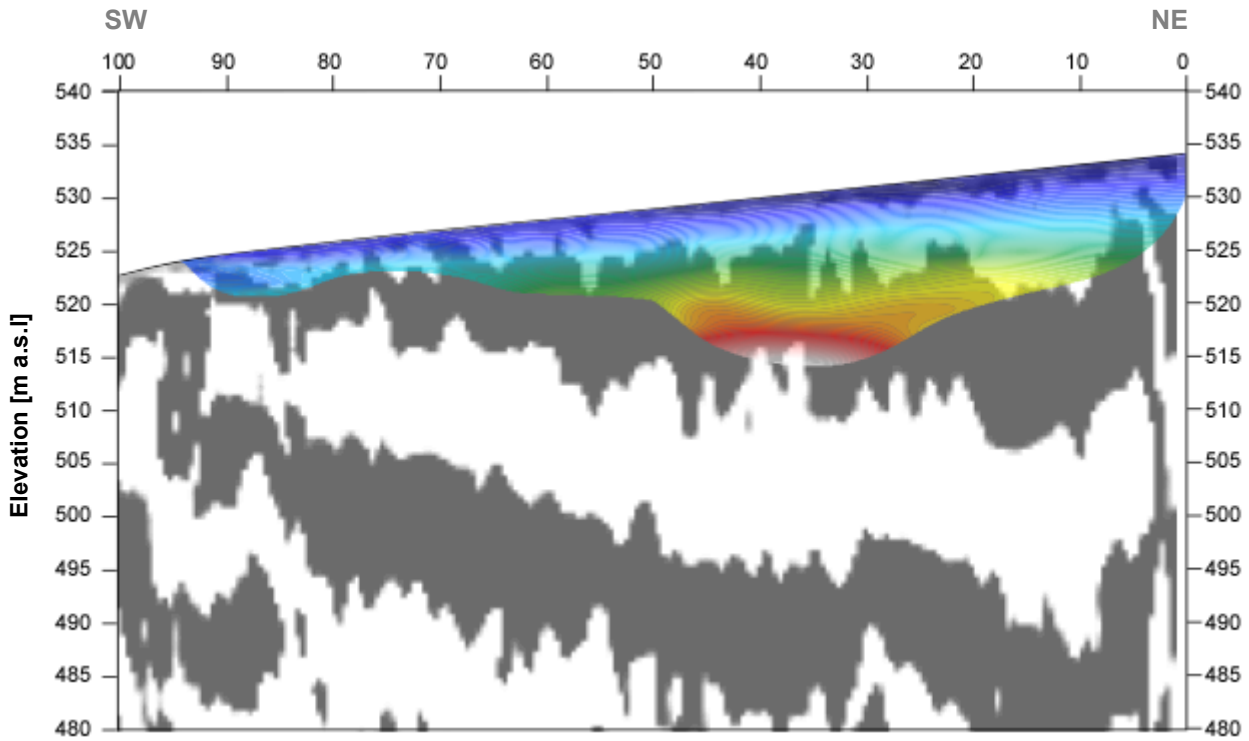

Fig. 3.4k Uninterpreted hybrid seismic section 09SN_15STEIN-P2: superimposed onto the seismic reflection section is the color encoded p-velocity field derived by refraction tomography (no vertical exaggeration).

4 DISCUSSION OF THE RESULTS

4.1 Summary and Validation of the Results

Compressional and shear wave velocity data from refraction seismic surveys both p-wave and s-wave and also the MASW survey data of profiles 09SN_15STEIN-1 and -2 are shown in Tab. 4.1 for the uppermost 30 m. The calculated shear wave velocity $v_{s(calc)}$ in Tab. 4.1 is derived by using a theoretical v_p/v_s-ratio of $\sqrt{3}$.

Depth	Vp1	Vp2	Vs1	Vs2	Vs1	Vs2	Vs1	Vs2
	meas	meas	calc	calc	meas	meas	MASW	MASW
0	427	374	195	247	204	216	251	272
1			192		210		243	267
2	480	509	236	277	233	294	241	304
3	585	643	274	338	271	371		
4	673	786	283	389	295	454	313	290
5	715	1082	291	413	304	625		
6	731	1251	299	422	313	723	340	246
7	756	1424	317	436	318	822		
8	812	1736		469	337	1002		320
9	902	1881	349	521	354	1086	348	
10	1002	2015	389	579	372	1163		
11	1103	2242	419	637	389	1295		478
12	1129	2342	428	652	411	1352	466	
13	1063	2454	428	614	450	1417		
14	1009	2723	440	583	467	1572		
15	1017	2901	462	587	475	1675		528
16	1040	3397	478	600	493	1961	538	
17	1090	3637	486	629	524	2100		
18	1169		492	675	545			
19	1255		502	724	579			
20			525		623			450
21			556		677		487	
22			588		779			
23			620		825			
24					856			
25			652		884			684
26			679					
27			705				708	
28								
29								
30								

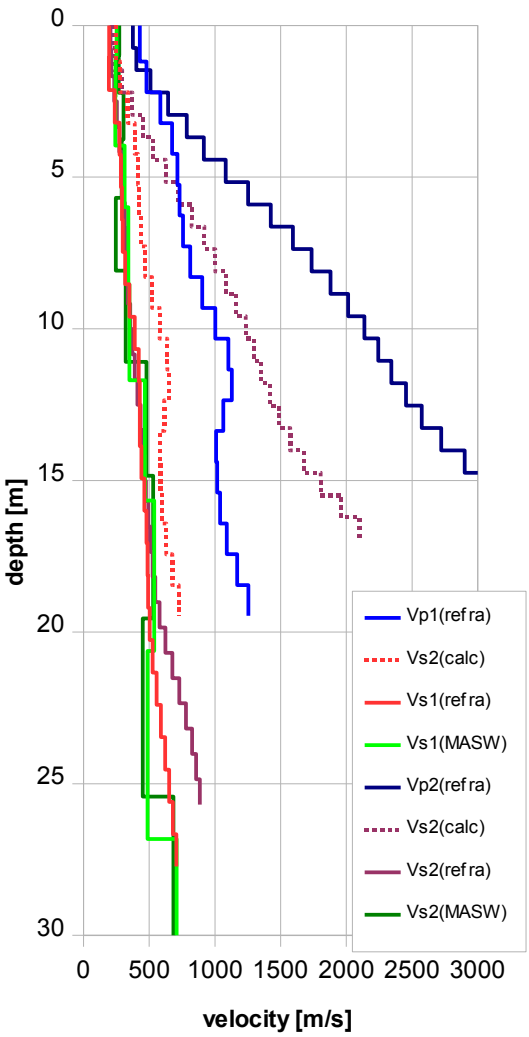

Tab. 4.1: Shear and compressional wave velocity model determined at the SED station STEIN.

Fig. 4.1: Graphic display of shear (continuous lines) and compressional (dotted lines) wave velocities determined at the SED station. In green colors MASW derived values, in blue values from p-wave and in red from s-wave refraction tomography.

4.2 Validation of the methods and their results

Due to methodological differences, v_s velocities derived by MASW analysis and by the refraction tomography technique may differ considerably. This is because MASW analysis cannot image small rock/soil inhomogeneities as a dispersion image with an array length of i.e. 40-m only yields one single v_s-value at each depth. On the other hand, refraction diving wave tomography results produce v_s-sections with a high lateral resolution, but fail to provide information at greater depths.

4.3 Error Estimates

The error estimates given in Tab. 4.3 below are relevant only in the context of this survey.

Surveying method	Type of result	Error estimate
v_s – refraction tomography	v_s – velocity field image	5%
MASW only "+" or only "-" values	v_s – velocity field image	5%
MASW (mean of "+" & "-" values)	v_s – velocity field image	5%
v_p – refraction tomography line 1	v_p – velocity field image	5%
v_p – refraction tomography line 2	v_p – velocity field image	not reliable
Reflection seismic surveying	Image of subsurface structures	n.a.

Tab. 4.3 Error estimates for the methods applied. Note that higher error estimates are to be taken into account with increasing depths.

The above error estimates are of a qualitative character only.

At the SED station STEIN (Stein a. Rh. SH), the refraction velocity images both from shear and compressional wave analysis show coincident structures on line 09SN_15STEIN-1. On line 09SN_15STEIN-2, it was not possible to evaluate the data by p-wave refraction tomography due to high level noise of vineyard works during the measurement period. The MASW figures are in the astonishingly same range as the values obtained from the shear wave diving wave refraction tomography surveys.

4.4 The Geophysical Interpretation

The most conclusive information about the subsurface structures is provided by the results of the hybrid seismic section (v_p-refraction tomography profiling and reflection seismic section) and confirmed by the evaluation results of the v_s-refraction tomography data.

As can be seen from the v_s and v_p refraction tomography sections in Fig. 3.2e/f & Fig. 3.4g/h, the topography of the bedrock surface is imaged vaguely on the profiles. The geological interpretation of the seismic events is shown in Fig. 4.2a. The fact that no hardrock is clearly imaged may be because of low contrast in impedance between Quarternary deposits and Tertiary sandstone. In the bedrock, no layering could be detected.

The relatively high velocities between profile meter 55 and 85 reflect possibly anthropogenic worked soil, i.e. fundaments.

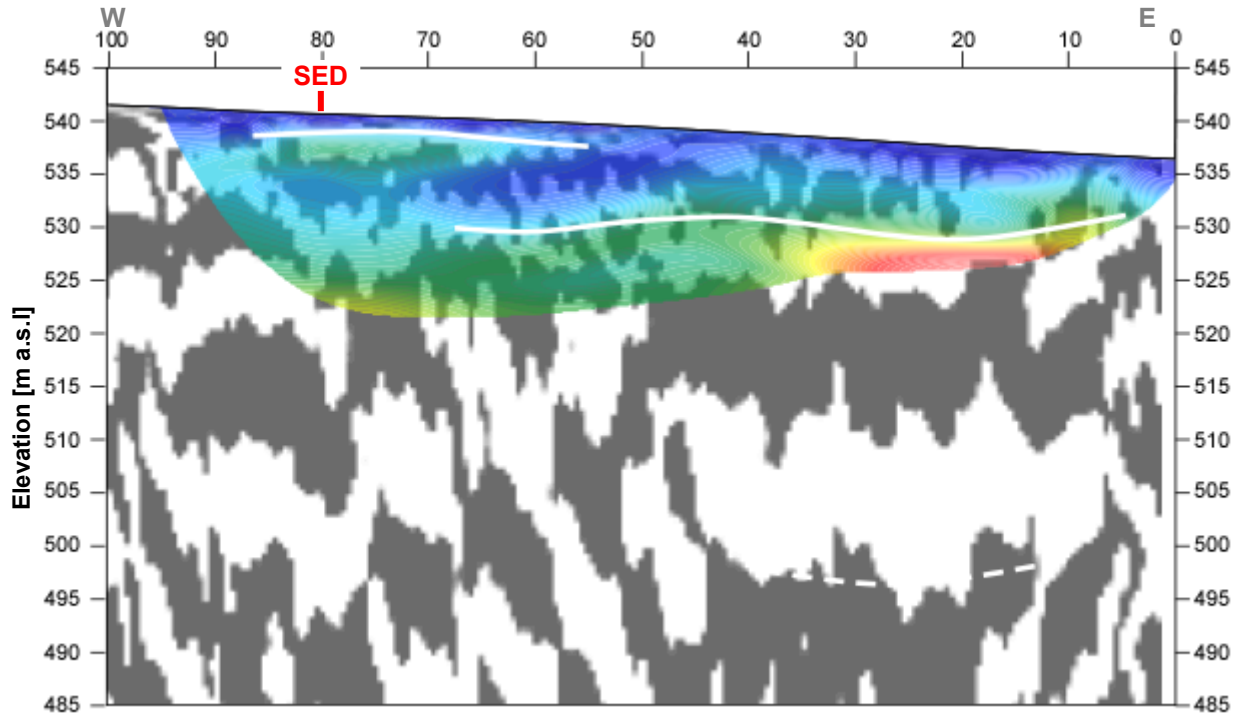

Fig. 4.2a Geophysical interpretation of the hybrid seismic section 09SN_15STEIN-P1. White lines denote layer boundaries, continuous line the bedrock surface.

The geological interpretation of the seismic events of line 09SN_15STEIN-2 is shown in Fig. 4.2a. A layering in the subsurface structures is imaged. Possible, that this reflect the layering of the sandstone, dipping to the Northeast. The bedrocks surface is imaged vaguely in a depth of 0 to 8 m, outcropping in the Southwest.

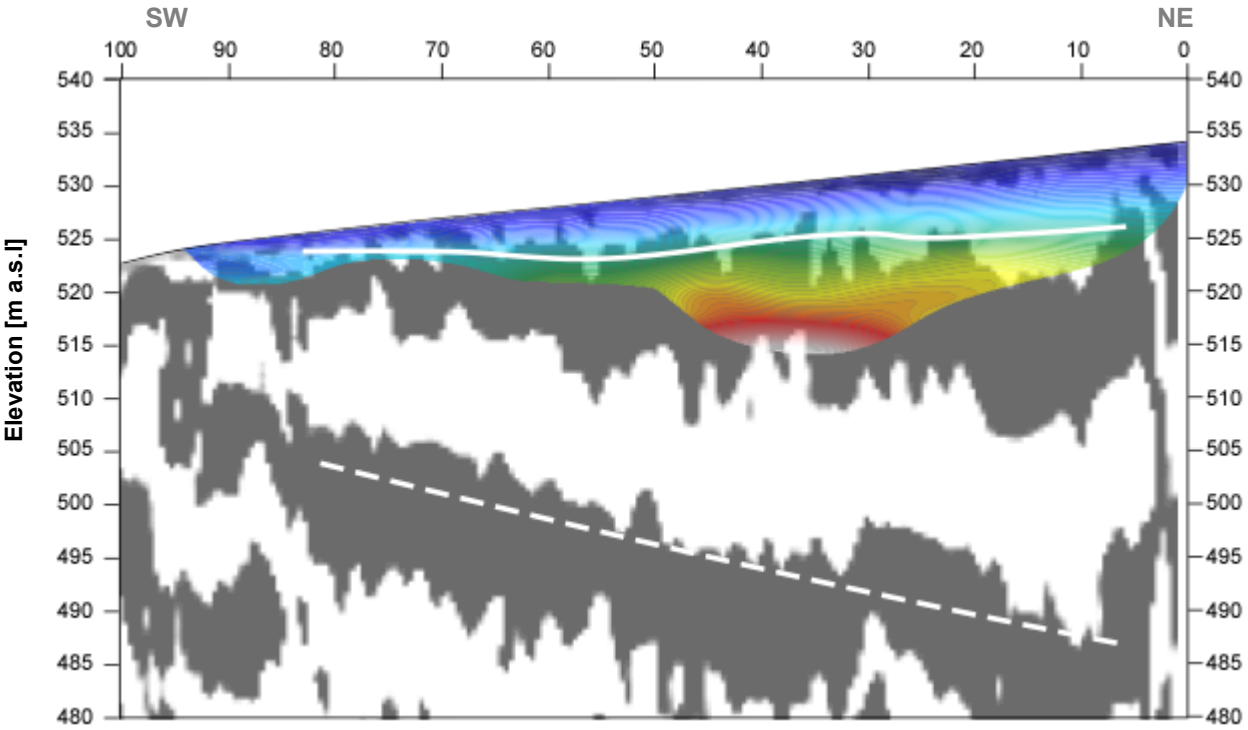

Fig. 4.2b Geophysical interpretation of the hybrid seismic section 09SN_15STEIN-P2. White lines denote layer boundaries, the continuous one marks the bedrock surface.

Remarkable are the very low velocities, both from shear compressional waves. The velocities at site STEIN are the lowest of all the SP2 measurements in PEGASOS Refinement Project done by GeoExpert ag.

5 SUMMARY AND CONCLUSIONS

- In May 2009 a combined seismic s- and p-wave survey was carried out at the SED earthquake monitoring station STEIN near Stein a. Rh. SH.
- The shear wave data have been evaluated by conventional diving wave refraction tomography techniques in order to derive the s-wave velocity field along the seismic line.
- The p-wave data have been processed
  - firstly to derive a 2D s-wave velocity field by using the MASW (**M**ultichannel **A**nalysis of **S**urface **W**aves) technique;
  - and secondly, according to the hybrid seismic data processing scheme for representing the subsurface structures in a combined reflection seismic section with the superimposed p-wave velocity field.
- The shear wave velocity range determined by the MASW method in the uppermost 30 meters spans from values of 241 m/s to 708 m/s.
- The scalar values derived by the MASW survey, valuable at the SED station (seismic line 09SN_15STEIN-M1); seismic line 09SN_15STEIN-M2) are the following:

line 1			line 2		
$v_{s,5}$	=	245 m/s	$v_{s,5}$	=	283 m/s
$v_{s,10}$	=	277 m/s	$v_{s,10}$	=	269 m/s
$v_{s,20}$	=	333 m/s	$v_{s,20}$	=	333 m/s
$v_{s,30}$	=	378 m/s	$v_{s,30}$	=	373 m/s
$v_{s,40}$	=	n/a	$v_{s,40}$	=	n/a

- The maximum refraction shear wave velocity derived is 856 m/s at a depth of 24 m.
- The maximum p-wave velocity determined from line 09SN_15STEIN-P1 is 1255 m/s at a depth of 19 m.
- The geophysical interpretation of the subsurface structures in this report are to be validated and incorporated into a comprehensive appraisal by a geologist familiar with the local geological setting.

Schwerzenbach, 3rd July 2009

Walter Frei
dipl. Natw. ETH
managing director

Lorenz Keller
dipl. Natw. ETH
project manager